SUPPORTING INFORMATION

Screening of Metal-Organic Frameworks for Carbon Dioxide Capture from Flue Gas using a Combined Experimental and Modeling Approach

A. Özgür Yazaydın[1], Randall Q. Snurr[1*], Tae-Hong Park[2], Kyoungmoo Koh[2], Jian Liu[3], M. Douglas LeVan[3], Annabelle I. Benin[4], Paulina Jakubczak[4], Mary Lanuza[4], Douglas B. Galloway[4], John J. Low[4], Richard R. Willis[4]

[1] *Department of Chemical & Biological Engineering, Northwestern University, Evanston, IL 60208*

[2] *Department of Chemistry, University of Michigan, Ann Arbor, Michigan 48109*

[3] *Department of Chemical & Biomolecular Engineering, Vanderbilt University, Nashville, TN 37235*

[4] *UOP LLC, a Honeywell Company, Des Plaines, IL 60017*

1. List of Metal-Organic Frameworks Investigated in this Work **S2**

2. General Information for Molecular Simulations **S3**

3. General Information for Experiments **S6**

4. Details of Simulations and Experiments for each MOF **S9**

5. Supplementary Results, Figures and Tables **S43**

6. Acknowledgments and Disclaimer **S50**

References **S51**

1. List of Metal-Organic Frameworks Investigated in this Work

HKUST-1[1]

$Pd(2\text{-pymo})_2$[2]

IRMOF-1[3]

IRMOF-3[4]

MOF-177[5]

Zn\DOBDC[6]

Ni\DOBDC[7]

Co\DOBDC [8]

Mg\DOBDC [9]

ZIF-8[10]

MIL-47[11]

UMCM-1[12]

UMCM-150[13]

$UMCM\text{-}150(N)_2$[14]

References refer to original publication of each MOF structure.

2. General Information for Molecular Simulations

Two different kinds of calculations were performed in this work. The first one is the DFT calculation for deriving partial charges of MOF atoms, and the second one is the grand canonical Monte Carlo (GCMC) simulation for obtaining the adsorption isotherms. DFT calculations are prerequisite for GCMC simulations, as the partial atomic charges are needed for GCMC.

2.1. DFT calculations

DFT calculations were performed on clusters isolated from the unit cell of each MOF, with the atomic coordinates taken from the experimental crystallographic data. These clusters included building units (e.g. metal-oxide corner and linker) representative of their respective unit cells. All DFT calculations were performed with the Gaussian 03[15] software using the B3LYP level of theory and the 6-31+G* basis set (except for the Pd atom in $Pd(2\text{-pymo})_2$ where the LanL2DZ effective core potential was used), and partial atomic charges were extracted using the ChelpG[16] method. Detailed information on clusters used for deriving partial charges for each MOF and resulting partial charges are given in section 4.

2.2. Grand canonical Monte Carlo (GCMC) simulations

2.2.1. Interaction potential

The interaction energy between the atoms was computed through the Coulomb and Lennard-Jones (LJ) potentials

$$V_{ij} = 4\varepsilon_{ij}\left[\left(\frac{\sigma_{ij}}{r_{ij}}\right)^{12} - \left(\frac{\sigma_{ij}}{r_{ij}}\right)^{6}\right] + \frac{q_i q_j}{4\varepsilon_0 r_{ij}}$$

where i and j are interacting atoms, and r_{ij} is the distance between atoms i and j. ε_{ij} and σ_{ij} are the LJ well depth and diameter, respectively. q_i and q_j are the partial charges of the interacting atoms, and ε_0 is the dielectric constant. LJ parameters between different types of sites were calculated using the Lorentz-Berthelot mixing rules.

2.2.2. MOF models

LJ parameters for all MOF atoms were taken from the DREIDING[17] force field or, if not available in DREIDING, then from the UFF[18] force field. Partial charges for MOF atoms were derived from DFT calculations as explained above and are tabulated in section 4 for each MOF type. Table S1 shows the LJ parameters for all atom types found in the MOFs we investigated in this work.

Table S1. LJ parameters for MOF atoms.

Atom type	σ (Å)	ε/k_B (K)	Force field
C	3.473	47.856	DREIDING
O	3.033	48.158	DREIDING
H	2.846	7.649	DREIDING
N	3.263	38.949	DREIDING
Zn	4.045	27.677	DREIDING
Cu	3.114	2.516	UFF
Ni	2.525	7.548	UFF
Co	2.559	7.045	UFF
Mg	2.6914	55.857	UFF
Pd	2.583	24.154	UFF
V	2.801	8.051	UFF

2.2.3. CO_2 Model

Partial charges and LJ parameters for CO_2 were taken from the TraPPE[19,20] force field. This force field has been fit to reproduce the vapor-liquid coexistence curves by Siepmann and co-workers. CO_2 molecule is modeled as a rigid and linear structure. Tables S2 shows the LJ parameters and partial charges for CO_2.

Table S2. LJ parameters and partial atomic charges for CO_2 atoms.

	O	C
σ (Å)	3.05	2.80
ε/k_B (K)	79.0	27.0
q (e)	-0.35	0.70

2.2.4. General GCMC simulation settings

All GCMC simulations included a 1.0×10^5 cycle equilibration period followed by a 1.0×10^5 cycle production run. A cycle consists of N Monte Carlo steps; where N is equal to the number of molecules (which fluctuates during a GCMC simulation). The Ewald sum technique was used to compute the electrostatic interactions. All simulations included random insertion, deletion and translation moves of guest molecules with equal probabilities. MOF atoms were held fixed at their crystallographic positions. A Lennard-Jones cutoff distance of 12.8 Å was used for all simulations. The number of unit cells used was different depending on the MOF type and is given in section 4 for each MOF. Simulations were performed at the temperature experimental data were available and ranged between 293 and 298 K. Fugacities needed to run the GCMC simulations were calculated using the Peng-Robinson equation of state. All simulated adsorption data reported in this work is the excess quantity, as it is the proper quantity for comparison with experimental data.[21] The isosteric heats of adsorption, Q_{st}, were estimated using the following formula[22]

$$Q_{st} = RT - \left(\frac{\partial \langle V \rangle}{\partial \langle N \rangle} \right)_T$$

where R is the gas constant, $\langle V \rangle$ is the average potential energy of the adsorbed phase, and $\langle N \rangle$ is the average number of molecules adsorbed. The formula above takes into consideration the fact that within the temperature (293 K - 298 K) and pressure (0.1 bar – 1 bar) ranges examined the residual enthalpy and the compressibility of CO_2 in the bulk phase are very close to 0 and 1, respectively, and, therefore, can be neglected.

2.3. Surface area, free volume and pore size distribution calculations

Geometric surface areas of the MOFs were calculated with the method reported by Düren et al.[23] by using a nitrogen probe with a diameter of 3.681 Å. We used the method described by Frost et al.[21] for the free volume calculations. Pore diameters were calculated by the method of Gelb et al.[24] The calculated quantities are reported in Table S34 for each MOF.

3. General Information for Experiments

In this section general information regarding sample preparation and CO_2 adsorption measurements is given. Experimental details for each MOF are given in section 4.

3.1. Sample preparation

All reagents and solvents employed were commercially available as follows and used as supplied without further purification. Sigma-Aldrich: *N, N'*-Dimethylformamide ≥ 99.8% (DMF), *N, N'*-Diethylformamide 99% (DEF), tetrahydrofuran ≥ 99% (THF), zinc nitrate hexahydrate 98% ($Zn(NO_3)_2*6H_2O$), copper nitrate hemipentahydrate 98% ($Cu(NO_3)_2*2.5H_2O$), nickel (II) nitrate hexahydrate ($Ni(NO_3)_2*6H_2O$), cobalt nitrate hexahydrate ($Co(NO_3)_2*6H_2O$), chromium(III) nitrate nonahydrate 99% ($Cr(NO_3)_3*9H_2O$), vanadium trichloride 97% (VCl_3), benzenedicarboxylic acid 98% (H_2BDC), 1,3,5-benzenetricarboxylic acid 95% (H_3BTC), 2-methylimidazole 99% (H-MeIM) 2,5-dihydroxyterephthalic acid 98% (DOBDC). Fisher: Methyl alcohol certified ACS (MeOH), dichloromethane certified ACS (CH_2Cl_2). STREM Chemicals: Nickel acetate tetrahydrate 98+% ($Ni(OAc)_2*4H_2O$), Cobalt acetate tetrahydrate 98+% ($Co(OAc)_2*4H_2O$). Alfa Aesar: Magnesium nitrate hexahydrate 98-102% ($Mg(NO_3)_2*6H_2O$). Acros: Triethylamine 99% (TEA). Aaper: ethyl alcohol 200 Proof (EtOH). 1,3,5-tris(4-carboxyphenyl)benzene (H_3BTB) was synthesized by Professor Adam Matzger's group at the University of Michigan.

3.2. Characterization Details

IRMOF-1, Ni\DOBDC, Co\DOBDC, Mg\DOBDC, ZIF-8, MIL-47. Powder X-ray diffraction (XRD) patterns of IRMOF-1, Ni\DOBDC, Co\DOBDC, Mg\DOBDC, ZIF-8, MIL-47 samples were obtained on a Scintag XDS 2000 (CuKα) over the range of 2-56º 2θ with a step size of 0.02º 2θ and a one second integration time per step. XRD patterns for these MOFs will be given in section 4 for the respective material. Sample surface area and pore volume measurements were determined from N_2 40-point isotherm data using a Micromeritics ASAP 2400 instrument. Samples were activated under dynamic vacuum overnight before analysis. See Table S3 below for details. The micropore volumes were calculated using the t-plot method.

UMCM-1. To obtain the powder X-ray diffraction (XRD) pattern of UMCM-1, a small amount of dried UMCM-1 was coated on a Nylon loop using mineral oil and mounted on a Rigaku R-Axis Spider diffractometer. Images were collected in transmission mode with χ set at 45°, ϕ rotating at 10°/min, and ω oscillating between 10° and 100° to minimize the effects of preferred orientation. Integration of the resulting image was performed in the AreaMax (2.0) software package with a step size of 0.1° in 2θ. The XRD pattern for UMCM-1 is given in section 4. Sample surface area and pore volume measurements were determined from volumetric

N_2 adsorption isotherm measured at 77 K in the range of $1.01325 \times 10^{-5} \leq P/P_0 \leq 1.01325$ bar with an Autosorb-1C outfitted with the micropore option by Quantachrome Instruments (Boynton Beach, Florida USA), running version 1.2 of the ASWin software package. UMCM-1 was charged into a sample cell and dried under vacuum (< 0.1 millitorr) at room temperature before analysis. See Table S3 below for details. The micropore volumes were calculated using the t-plot method.

Table S3. Summary of surface area measurements

Sample	Pretreatment	Vacuum activation (overnight in ^oC)	BET SA (m^2/g)	Langmuir SA (m^2/g)	TPV (cc/g)	MiPV (cc/g)
IRMOF-1	300 deg C, 6h (nitrogen)	125	1892	2784	2.345	0.767
Ni\DOBDC	none	150	936	1356	0.495	0.476
Co\DOBDC	none	170	957	1388	0.498	0.487
ZIF-8	none	300	1135	1768	0.630	0.626
MIL-47	275 deg C, 21.5h (air)	150	600	872	0.338	0.302
UMCM-1	none	25 (2h only)	4034	5182	2.30	0.516

3.3. Procedure for CO_2 adsorption measurements

IRMOF-1, Ni\DOBDC, Co\DOBDC, Mg\DOBDC, ZIF-8, MIL-47. The isotherms of IRMOF-1, Ni\DOBDC, Co\DOBDC, Mg\DOBDC, ZIF-8, MIL-47 samples were measured using one of two Rubotherm gravimetric systems (VTI Corp.). Before the CO_2 adsorption measurements, samples were regenerated in the gravimetric system under high vacuum (about 10^{-7} mbar) at preset temperatures, which varied depending on the MOF. After regeneration, the sample was cooled using flowing dry helium. Adsorption isotherm data were corrected for buoyancy using helium as a probe gas. The CO_2 isotherms were generated at 25 °C with various sized pressure steps.

Regeneration temperatures and times, all for the high vacuum, were as follows. These were sufficient to obtain stable, minimum weights. The Ni\DOBDC and Co\DOBDC samples were regenerated at 125 ^oC for 3 hours. The Mg\DOBDC sample was regenerated at 250 ^oC for 5 hours. The ZIF-8 sample was regenerated at room temperature for 5 hours and then at 260 ^oC overnight. IRMOF-1 and MIL-47 were regenerated at 125 ^oC for 8h. The latter two samples also underwent a second 125 °C heating for 30 minutes under vacuum to remove all of the helium.

UMCM-1. The CO_2 isotherm of UMCM-1 sample was measured volumetrically at 25 ^{o}C in the range of $1.01325 \times 10^{-5} \leq P/P_0 \leq 1.01325$ bar with an Autosorb-1C outfitted with the micropore option by Quantachrome Instruments (Boynton Beach, Florida USA), running version 1.2 of the ASWin software package. UMCM-1 was charged into a sample cell and dried under vacuum (< 0.1 millitorr) at room temperature for 2 hours before CO_2 adsorption measurement.

4. Details of Simulations and Experiments for each MOF

4.1. HKUST-1

Partial atomic charges

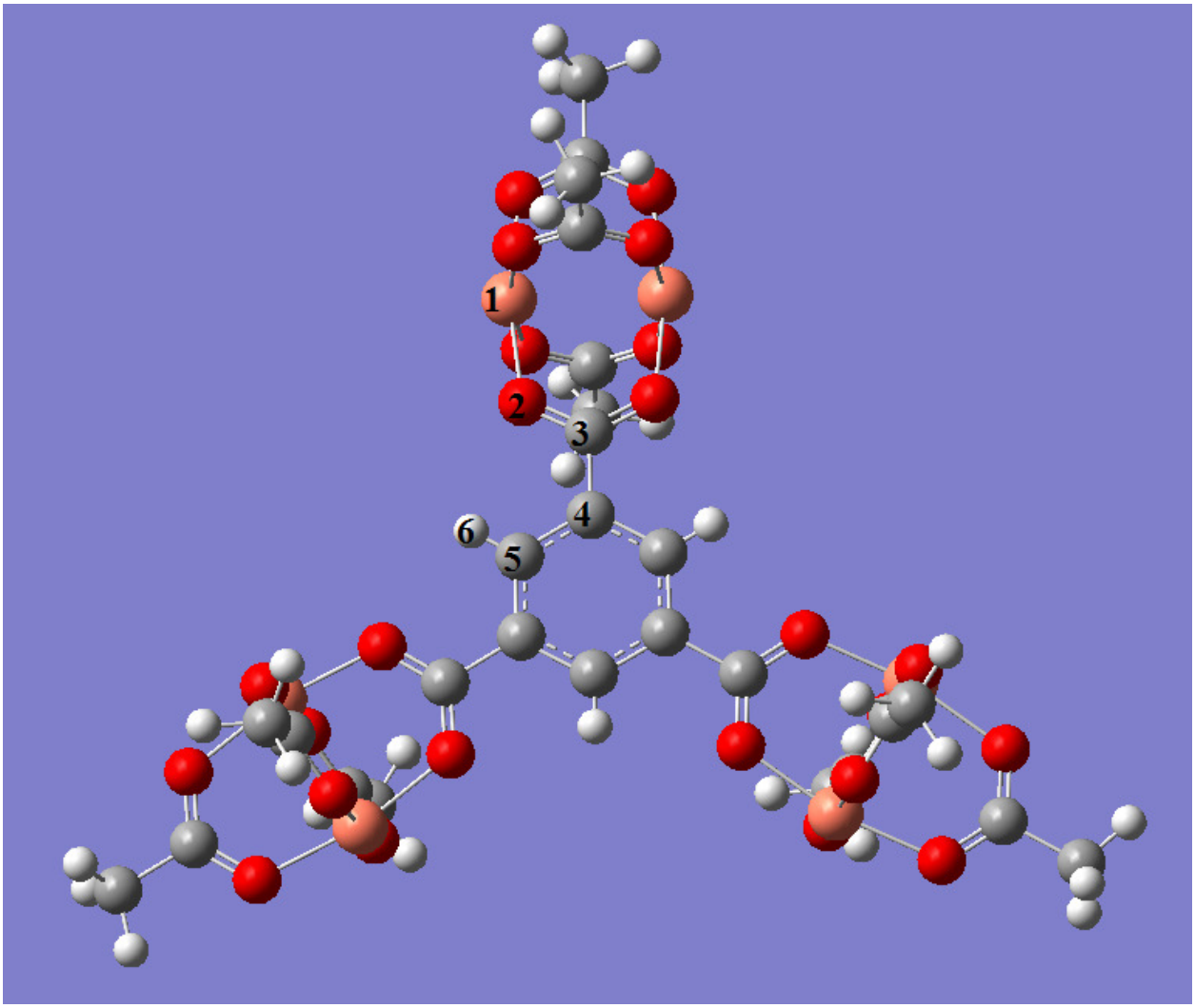

Figure S1. Cluster ($Cu_6C_{36}O_{24}H_{30}$) used for deriving partial charges on HKUST-1 atoms.

Table S4. Partial atomic charges for HKUST-1 atoms.

Atom no	1	2	3	4	5	6
Charge (e)	1.13 (Cu)	-0.645 (O)	0.741 (C)	-0.07 (C)	-0.091 (C)	0.145 (H)

Table S5. GCMC simulation details for HKUST-1.

Number of unit cells	Cut-off distance (Å)	Temperature (K)	Coordinates
1x1x1 = 1	12.8	295	Chui et al. 1998[1]

Experimental details

Experimental CO_2 adsorption data were taken from the work of Wang et al. 2002.[25] ‡ For Figures 1 and 2 in the main text, experimental CO_2 data at 0.1 bar, 0.5 bar, and 1 bar were estimated by interpolation or extrapolation of the experimental data points.

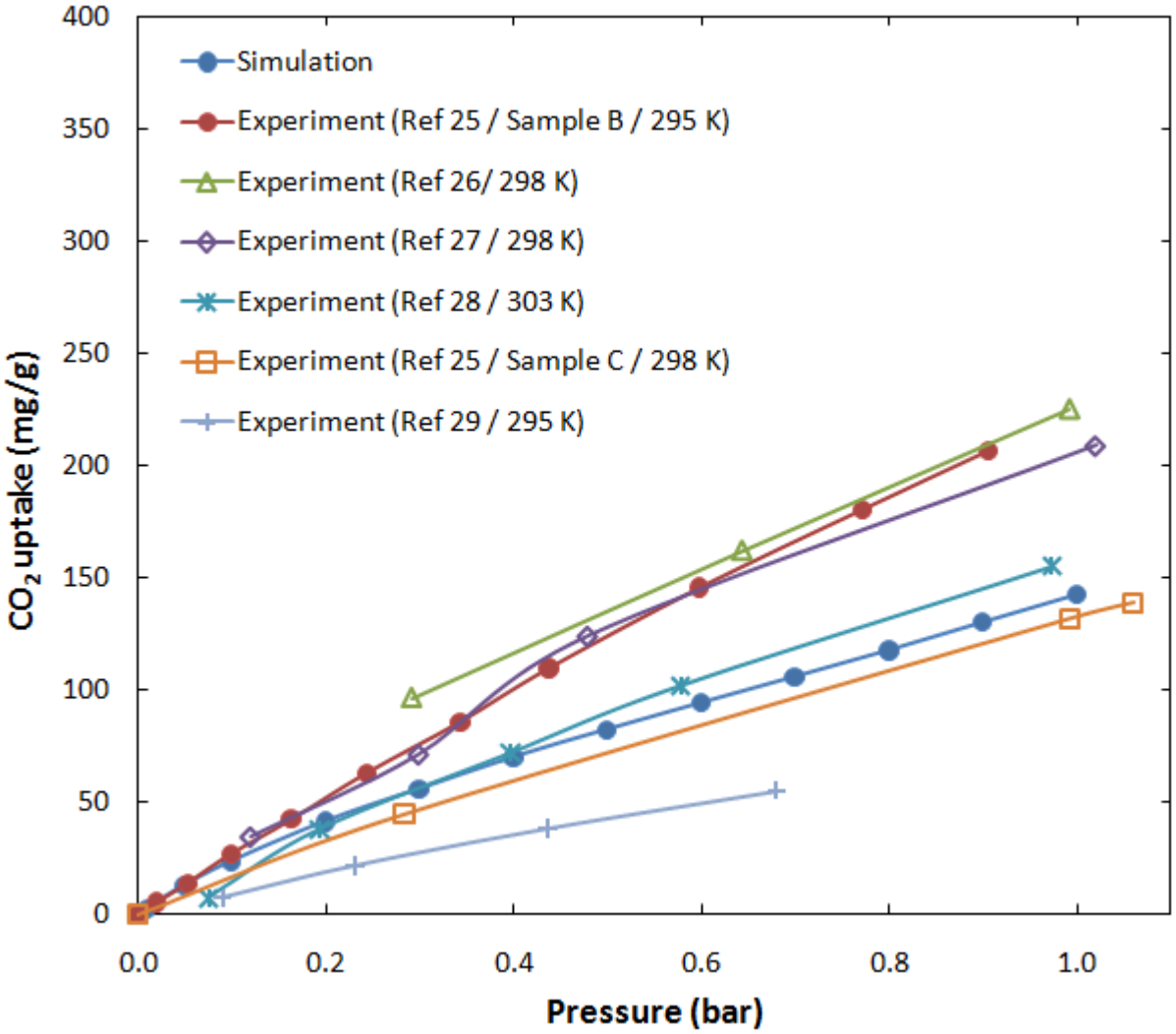

Figure S2. Comparison of simulated (295 K) and experimental CO_2 adsorption isotherms in HKUST-1. Lines are drawn to guide the eye.

‡ Our simulated CO_2 isotherms in HKUST-1 fall in the range of the experimental isotherms reported in the literature as shown in Figure S2. The variations in the experimental data are probably due to differences in the MOF samples, either due to sample preparation or activation. For Figures 1 and 2 in the main text, the data from Wang et al. 2002[25] (red circles above) were chosen because they showed one of the highest CO_2 capacities in HKUST-1 and had the most data points within the pressure range of interest. For other MOFs where more than one set of experiments were available in the literature, we followed a similar convention for choosing the data to use in Figures 1 and 2. This was done to provide an objective comparison.

4.2. $Pd(2\text{-pymo})_2$

Partial atomic charges

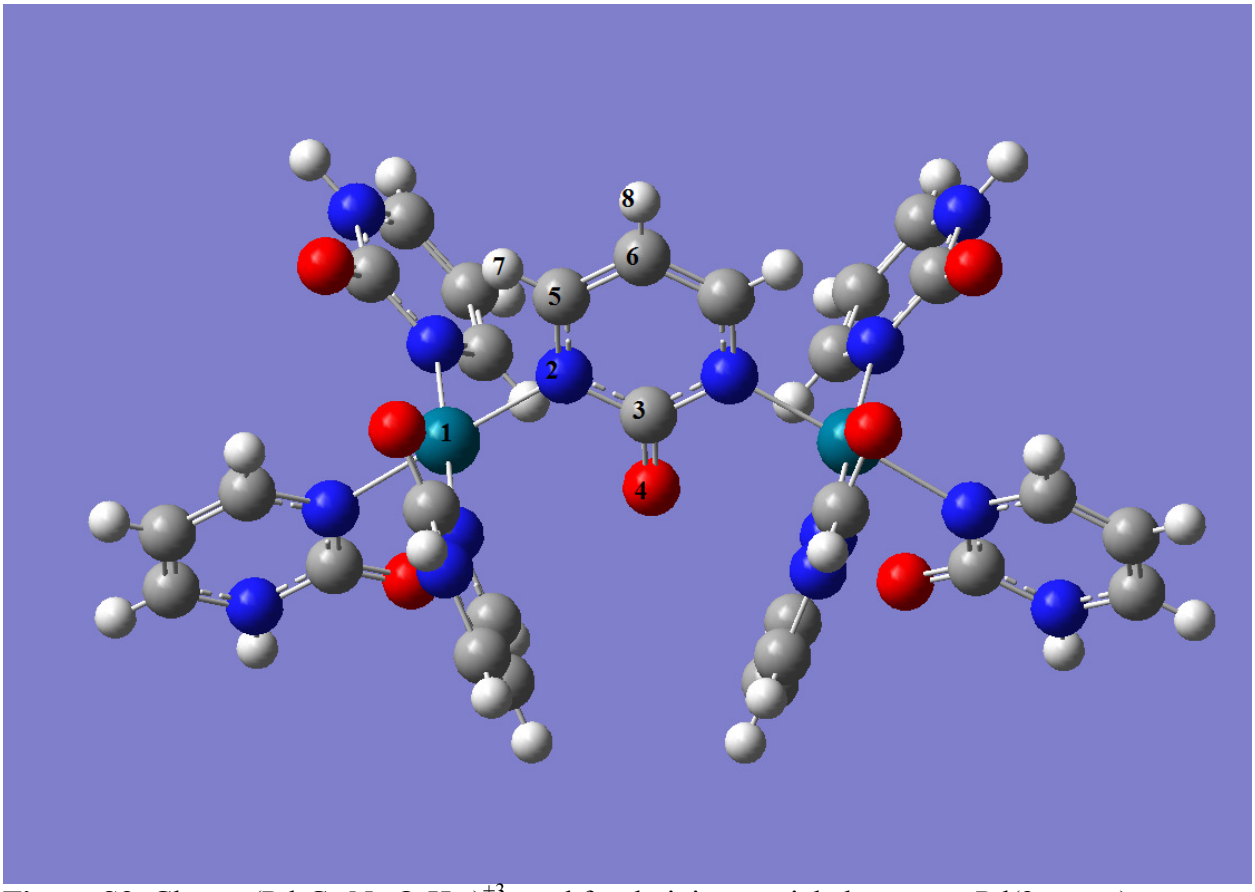

Figure S3. Cluster $(Pd_2C_{28}N_{14}O_7H_{28})^{+3}$ used for deriving partial charges on $Pd(2\text{-pymo})_2$ atoms.

Table S6. Partial atomic charges for $Pd(2\text{-pymo})_2$ atoms.

Atom no	**1**	**2**	**3**	**4**	**5**	**6**	**7**	**8**
Charge (e)	0.298 (Pd)	-0.247 (N)	0.595 (C)	-0.664 (O)	0.102 (C)	-0.33 (C)	0.17 (H)	0.2 (H)

Table S7. GCMC simulation details for $Pd(2\text{-pymo})_2$.

Number of unit cells	**Cut-off distance (Å)**	**Temperature (K)**	**Coordinates**
2x2x2 = 8	12.8	293	Navarro et al. 2006[2]

$Pd(2\text{-pymo})_2$ has pores that are accessible to CO_2 molecules in GCMC simulations but not accessible in adsorption experiments. This is due to the fact that in GCMC simulations molecules can be directly inserted in to the pores, whereas, in reality molecules must diffuse through the

pores. In our GCMC simulations, pores that are not experimentally accessible to CO_2 molecules in $Pd(2\text{-pymo})_2$ were blocked by ghost atoms.

Experimental details

Experimental CO_2 adsorption data were taken from the work of Navarro et al. 2006.[2] For Figures 1 and 2 in the main text, experimental CO_2 data at 0.1 bar, 0.5 bar, and 1 bar were estimated by interpolation or extrapolation of the experimental data points.

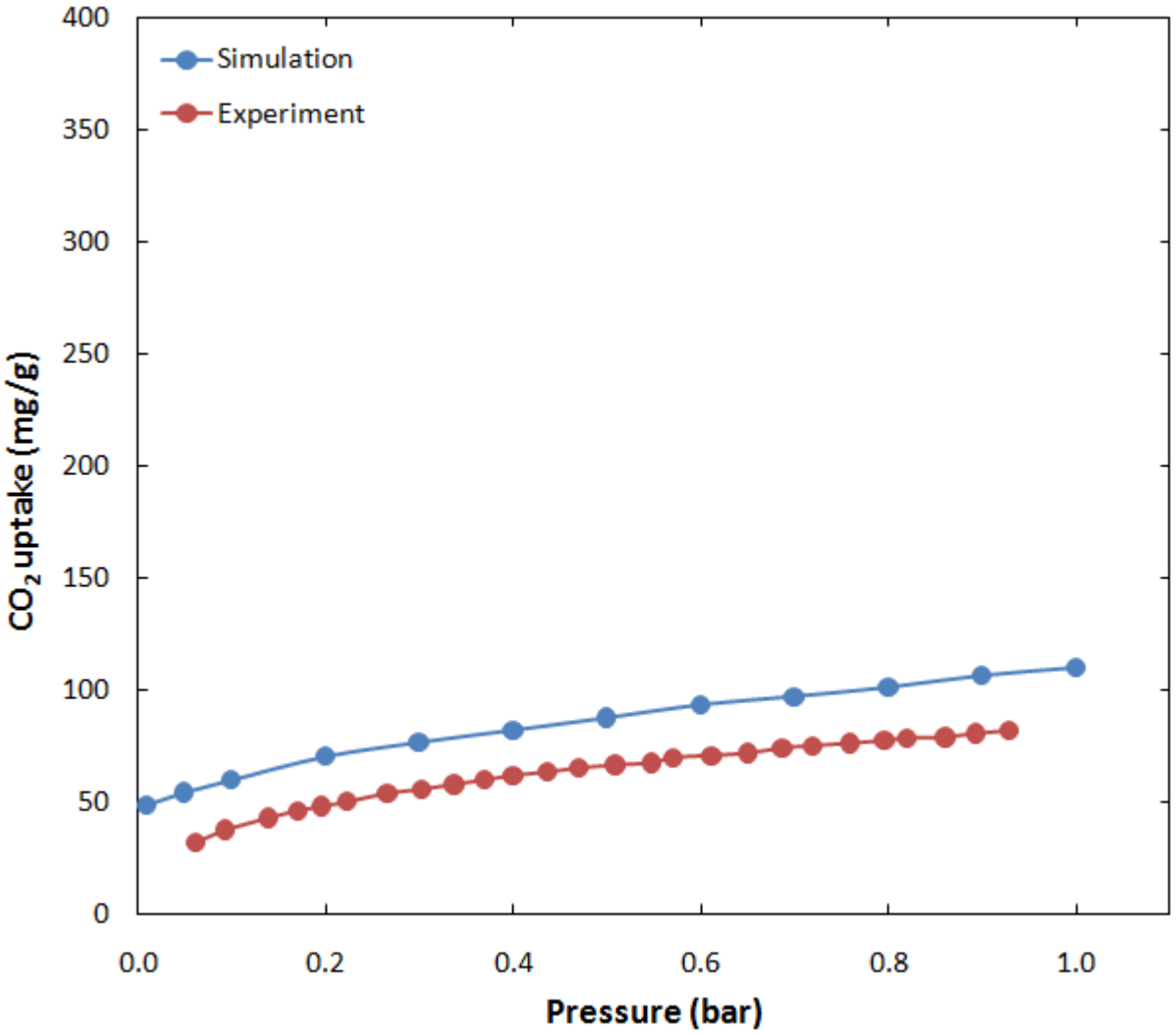

Figure S4. Comparison of simulated and experimental CO_2 adsorption isotherms in $Pd(2\text{-pymo})_2$ at 293 K. Lines are drawn to guide the eye.

4.3. IRMOF-1

Partial atomic charges

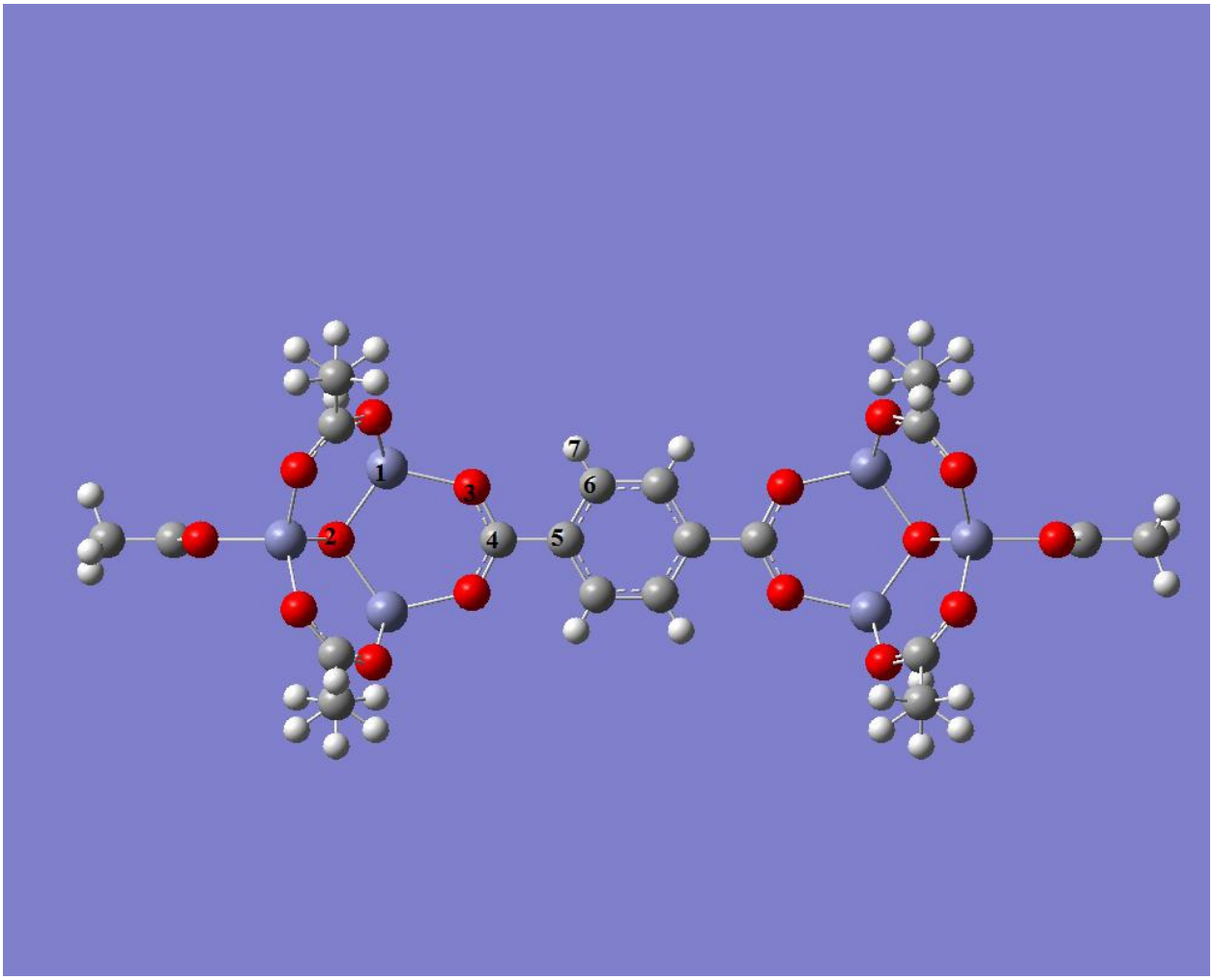

Figure S5. Cluster ($Zn_8C_{28}O_{28}H_{34}$) used for deriving partial charges on IRMOF-1 atoms. Cluster was terminated with methyl groups to minimize end effects.

Table S8. Partial atomic charges for IRMOF-1 atoms.

Atom no	1	2	3	4	5	6	7
Charge (e)	1.333 (Zn)	-1.564 (O)	-0.641 (O)	0.558 (C)	0.106 (C)	-0.167 (C)	0.162 (H)

Table S9. GCMC simulation details for IRMOF-1.

Number of unit cells	Cut-off distance (Å)	Temperature (K)	Coordinates
1x1x1 = 1	12.8	298	Li et al. 1999[3]

Experimental details

IRMOF-1, $Zn_4O(BDC)_3$, was synthesized according to the literature procedure.[30] The crystals were collected by repeated centrifugation and thorough DMF washing (3x, 1 hr each) followed by dry acetone washing (4-5 times, 4-5 d each). The white powder was then dried at 100 °C in a furnace with flowing nitrogen for at least 4 hours. All samples were stored in a desiccator to avoid moisture adsorption. Before gas adsorption analysis, IRMOF-1 was heated to 125 °C under dynamic vacuum for 16 hours. CO_2 adsorption data for IRMOF-1 were collected according to the procedure described in section 3. For Figures 1 and 2 in the main text, experimental CO_2 data at 0.1 bar, 0.5 bar, and 1 bar were estimated by interpolation or extrapolation of the experimental data points.

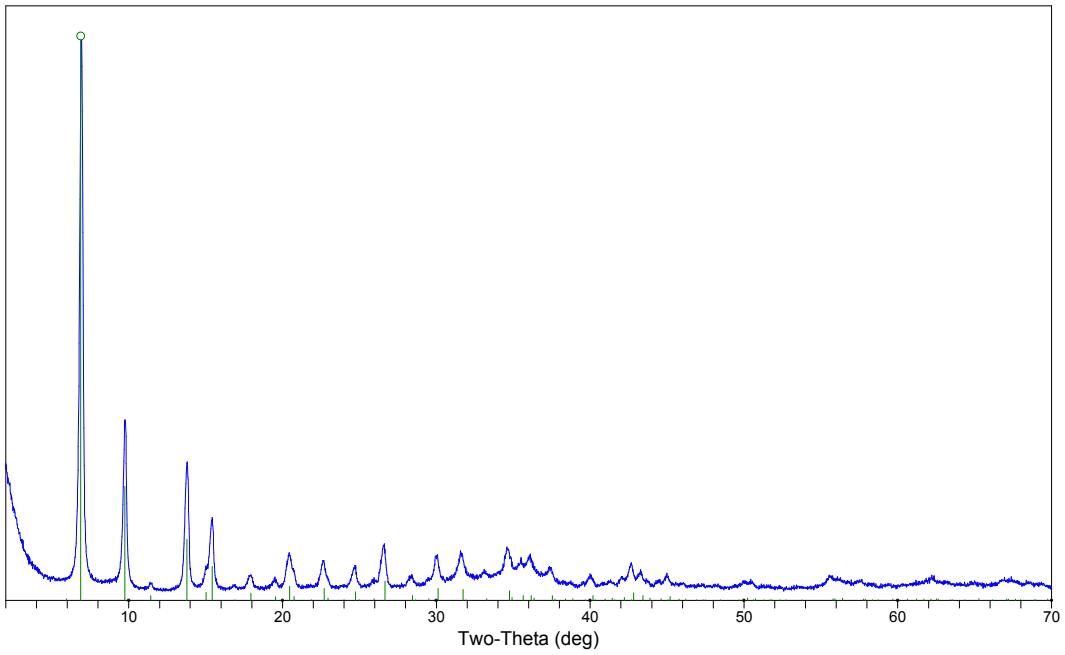

Figure S6. Powder x-ray diffraction (XRD) pattern for IRMOF-1. Sticks represent simulated powder patterns from data reported in the literature.

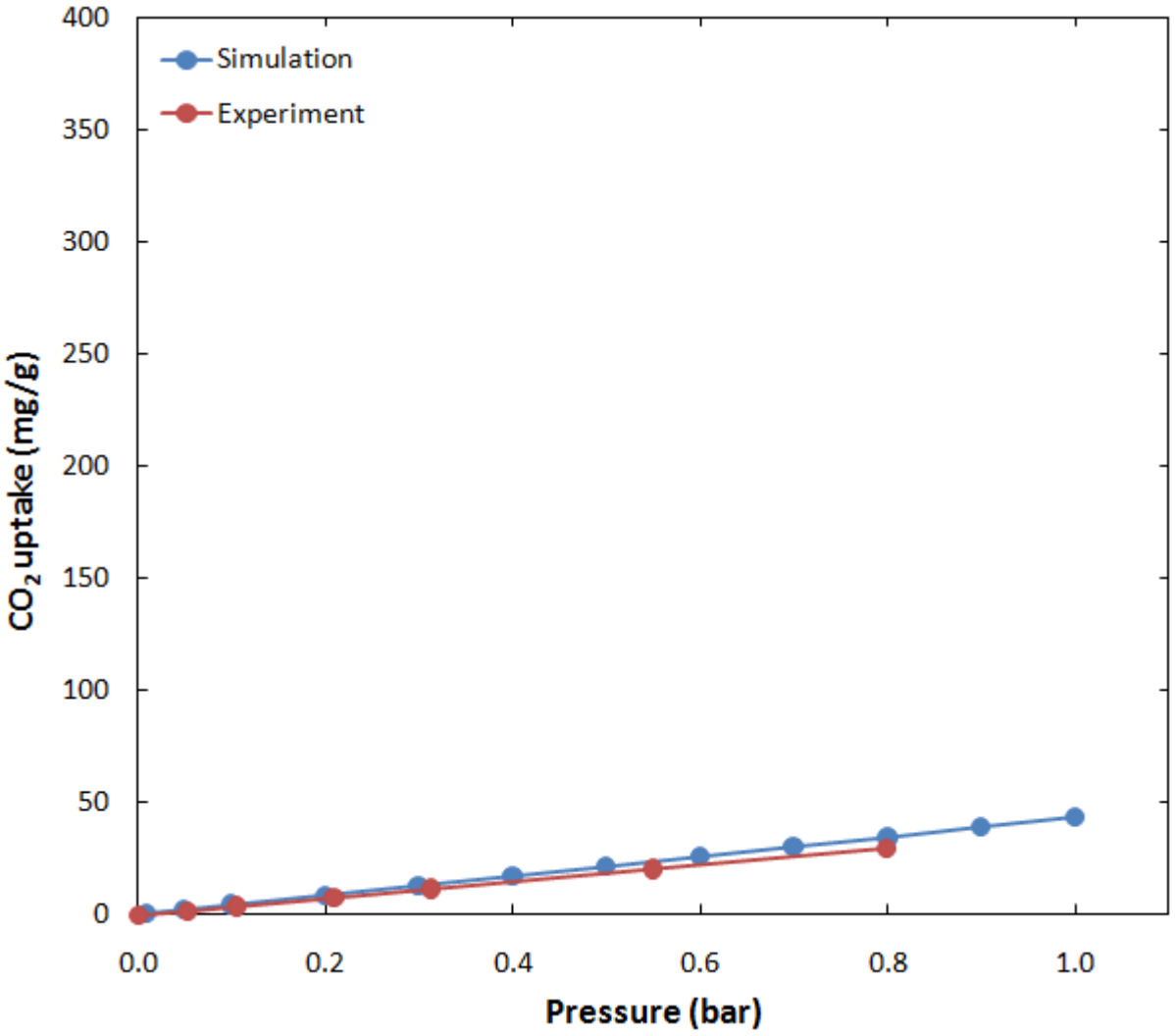

Figure S7. Comparison of simulated and experimental CO_2 adsorption isotherms in IRMOF-1 at 298 K. Lines are drawn to guide the eye.

4.4. IRMOF-3

Partial atomic charges

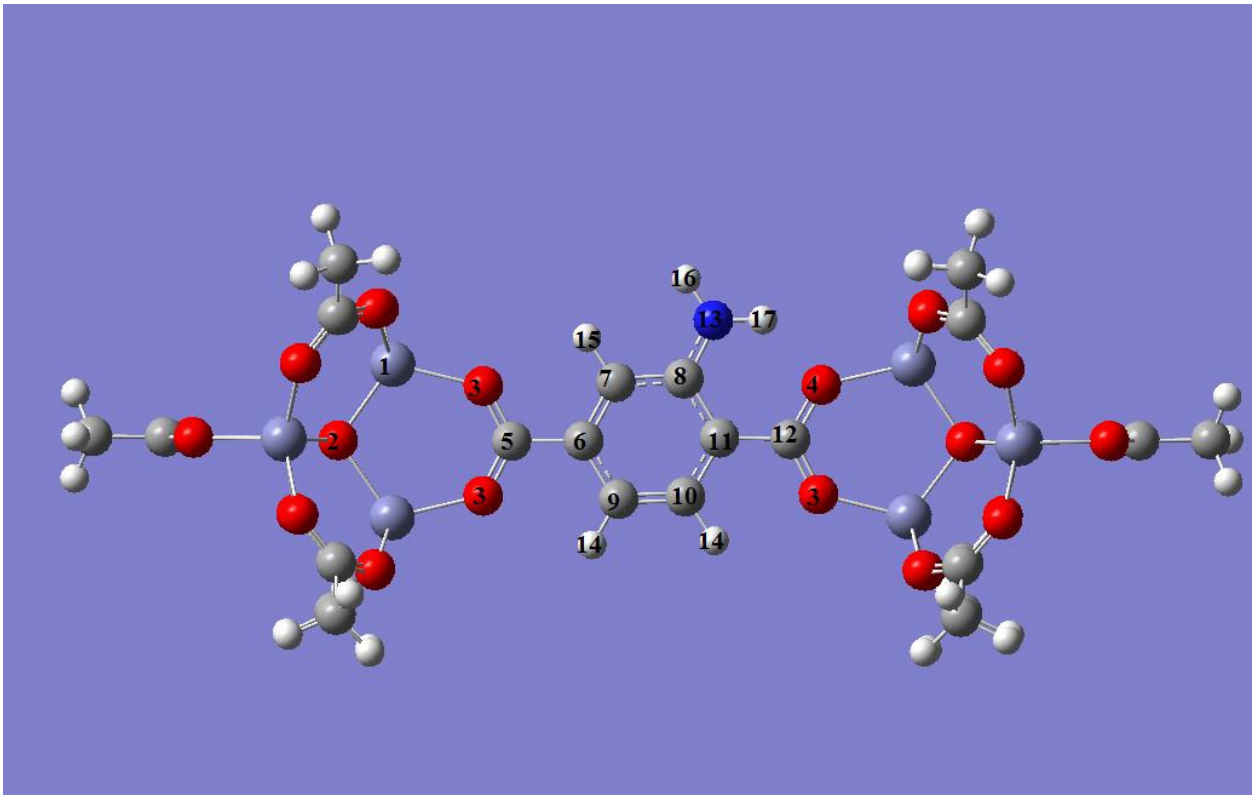

Figure S8. Cluster ($Zn_8C_{28}N_1O_{28}H_{35}$) used for deriving partial charges on IRMOF-3 atoms.

Table S10. Partial atomic charges for IRMOF-3 atoms.

Atom no	**1**	**2**	**3**	**4**	**5**	**6**
Charge (e)	1.387 (Zn)	-1.624 (O)	-0.679 (O)	-0.721 (O)	0.629 (C)	0.193 (C)
Atom no	**7**	**8**	**9**	**10**	**11**	**12**
Charge (e)	-0.438 (C)	0.554 (C)	-0.297 (C)	-0.114 (C)	-0.163 (C)	0.679 (C)
Atom no	**13**	**14**	**15**	**16**	**17**	
Charge (e)	-0.962 (N)	0.159 (H)	0.201 (H)	0.401 (H)	0.449 (H)	

Table S11. GCMC simulation details for IRMOF-3.

Number of unit cells	**Cut-off distance (Å)**	**Temperature (K)**	**Coordinates**
1x1x1 = 1	12.8	298	Eddaoudi et al. 2002[4]

Experimental details

Experimental CO_2 adsorption data were taken from the work of Millward et al. 2005.[31] For Figures 1 and 2 in the main text, experimental CO_2 data at 0.1 bar, 0.5 bar, and 1 bar were estimated by drawing a straight line between zero bar and the lowest pressure point in Millward et al.'s data, 1.1 bar. This is justified since the CO_2 adsorption is expected to show a linear profile at this pressure region.

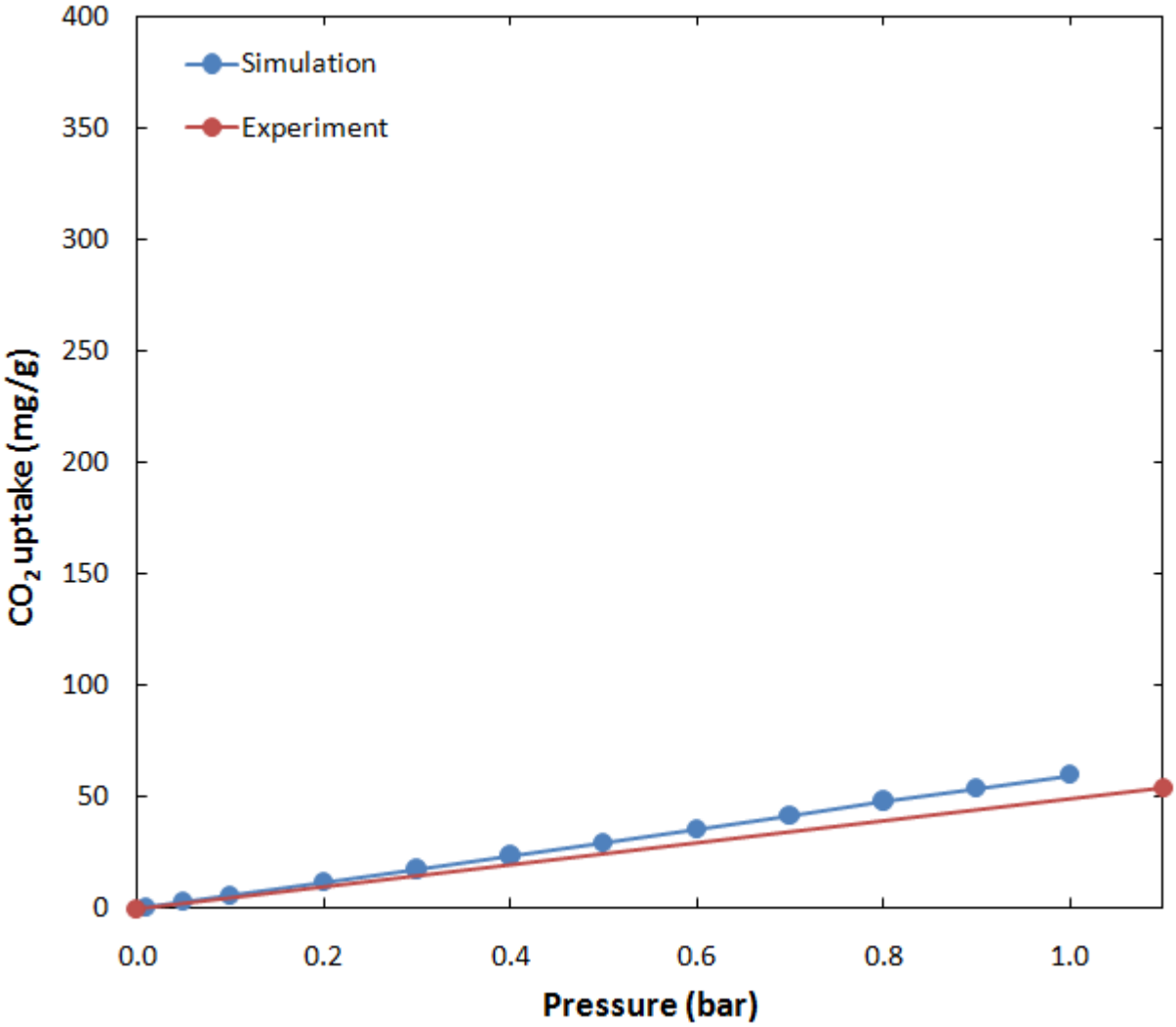

Figure S9. Comparison of simulated and experimental CO_2 adsorption isotherms in IRMOF-3 at 298 K. Lines are drawn to guide the eye.

4.5. MOF-177

Partial atomic charges

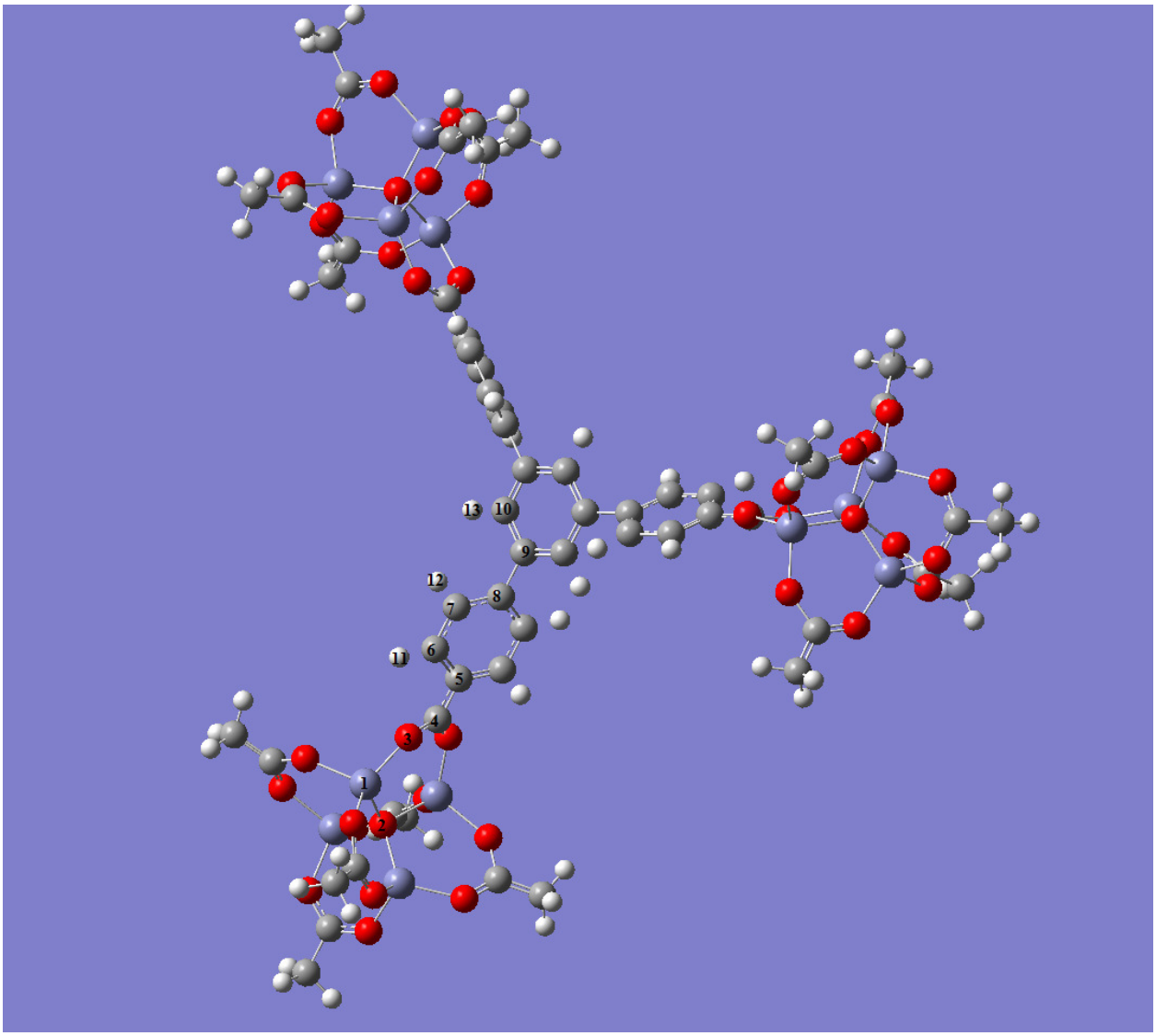

Figure S10. Cluster ($Zn_{12}C_{57}O_{41}H_{60}$) used for deriving partial charges on MOF-177 atoms.

Table S12. Partial atomic charges for MOF-177 atoms.

Atom no	**1**	**2**	**3**	**4**	**5**	**6**
Charge (e)	1.454 (Zn)	-1.670 (O)	-0.746 (O)	0.644 (C)	0.21 (C)	-0.214 (C)
Atom no	**7**	**8**	**9**	**10**	**11**	**12**
Charge (e)	-0.172(C)	0.144 (C)	0.123 (C)	-0.24 (C)	0.173 (H)	0.119 (H)
Atom no	**13**					
Charge (e)	0.108 (H)					

Table S13. GCMC simulation details for MOF-177.

Number of unit cells	Cut-off distance (Å)	Temperature (K)	Coordinates
1x1x1 = 1	12.8	298	Chae et al. 2004[5]

Experimental details

Experimental CO_2 adsorption data were taken from the work of Millward et al. 2005.[31] For Figures 1 and 2 in the main, experimental CO_2 data at 0.1 bar, 0.5 bar, and 1 bar were estimated by drawing a straight line between zero bar and the lowest pressure point in Millward et al.'s data, 1.0 bar. This is justified since the CO_2 adsorption is expected to show a linear profile at this pressure region.

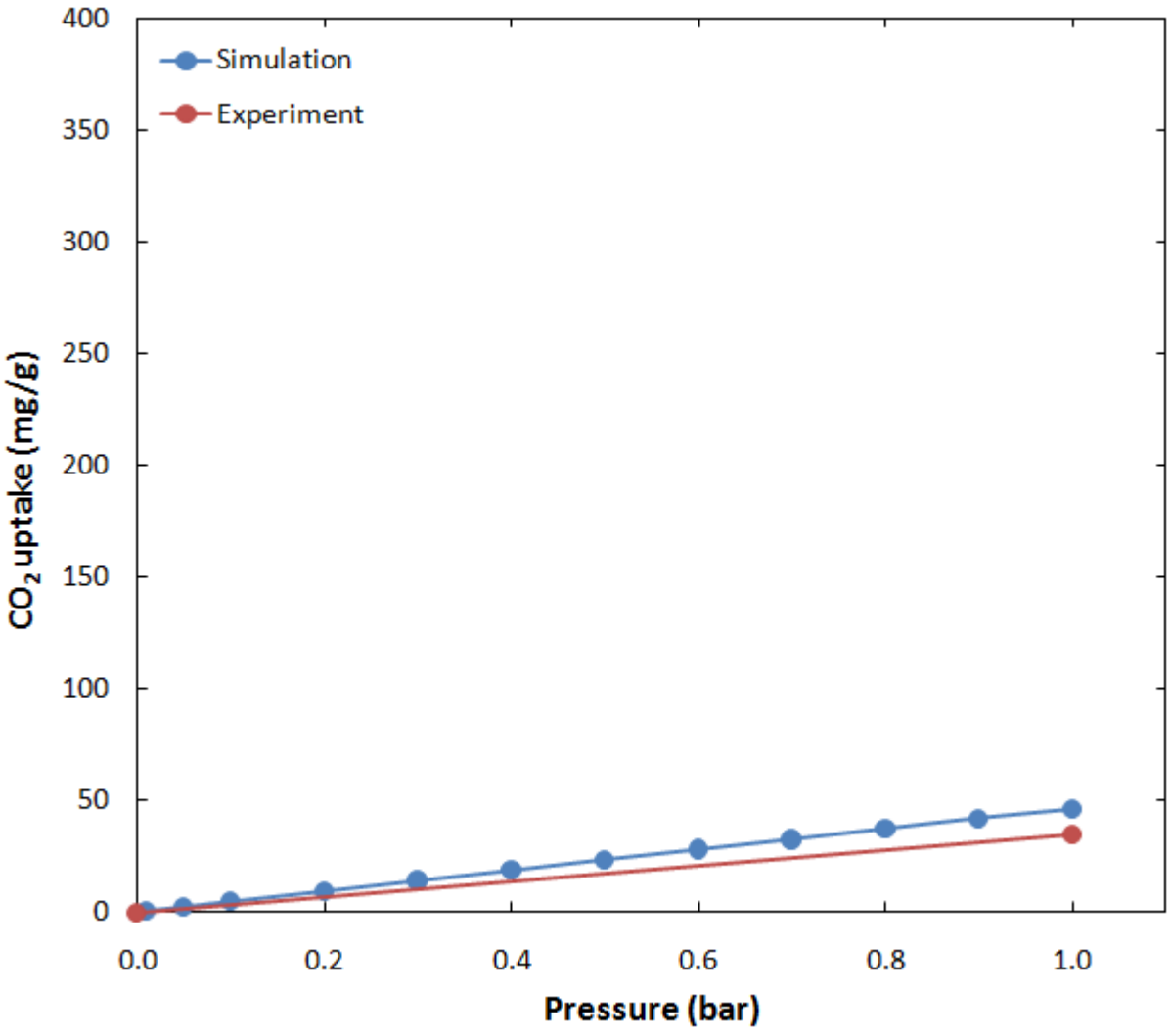

Figure S11. Comparison of simulated and experimental CO_2 adsorption isotherms in MOF-177 at 298 K. Lines are drawn to guide the eye.

3.6. Zn\DOBDC

Partial atomic charges

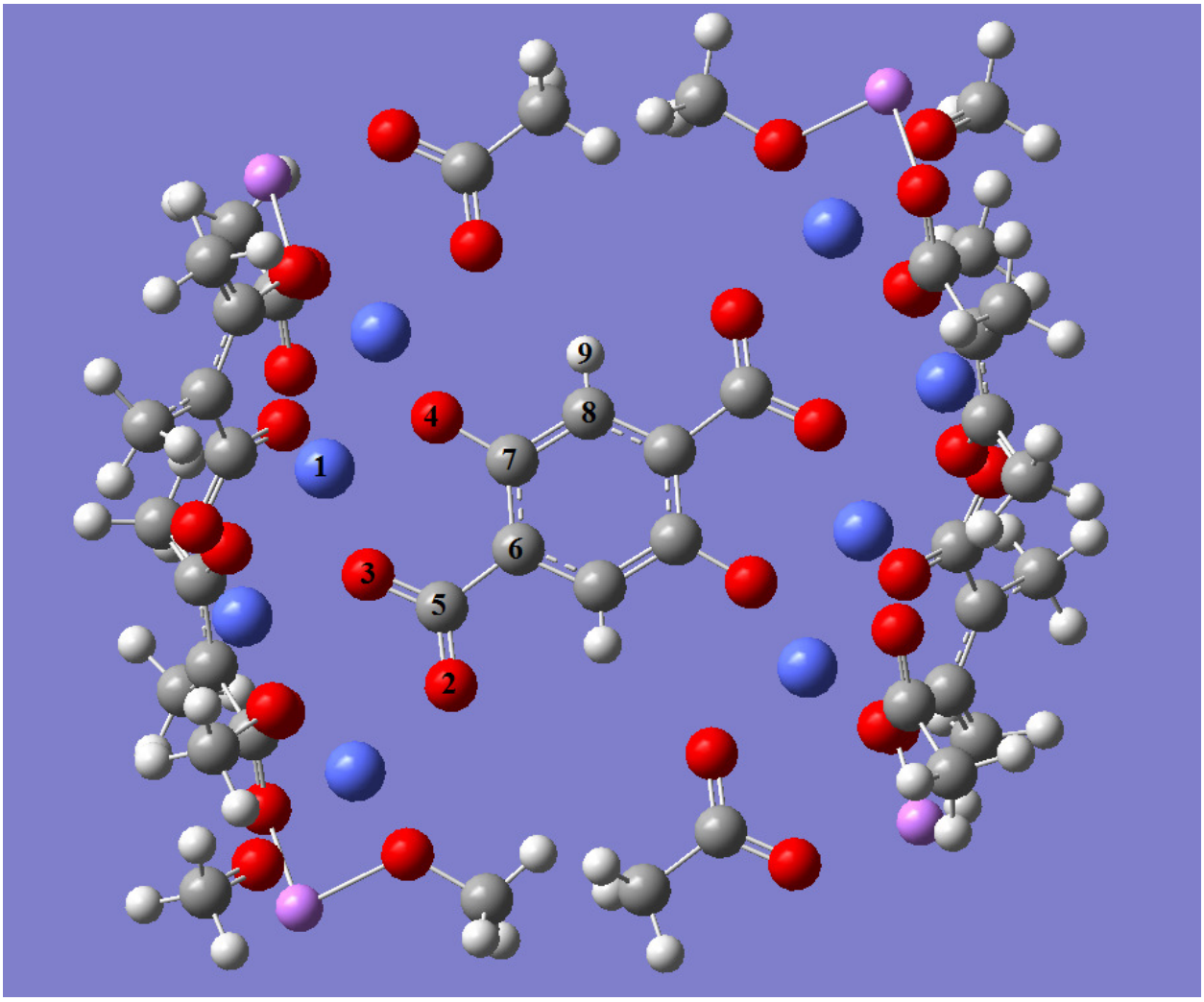

Figure S12. Cluster ($Zn_8C_{42}O_{32}H_{56}Li_4$) used for deriving partial charges on Zn\DOBDC atoms.

Table S14. Partial atomic charges for Zn\DOBDC atoms.

Atom no	**1**	**2**	**3**	**4**	**5**	**6**
Charge (e)	1.206 (Zn)	-0.670 (O)	-0.659 (O)	-0.702 (O)	0.767 (C)	-0.292 (C)
Atom no	**7**	**8**	**9**			
Charge (e)	0.325 (C)	-0.147 (C)	0.172 (H)			

Table S15. GCMC simulation details for Zn\DOBDC.

Number of unit cells	**Cut-off distance (Å)**	**Temperature (K)**	**Coordinates**
2x2x4 = 16	12.8	296	Rowsell et al. 2006[6]

Experimental details

Experimental CO_2 adsorption data were taken from the work of Caskey et al. 2008.[9] For Figures 1 and 2 in the main text, experimental CO_2 data at 0.1 bar, 0.5 bar, and 1 bar were estimated by interpolation or extrapolation of the experimental data points.

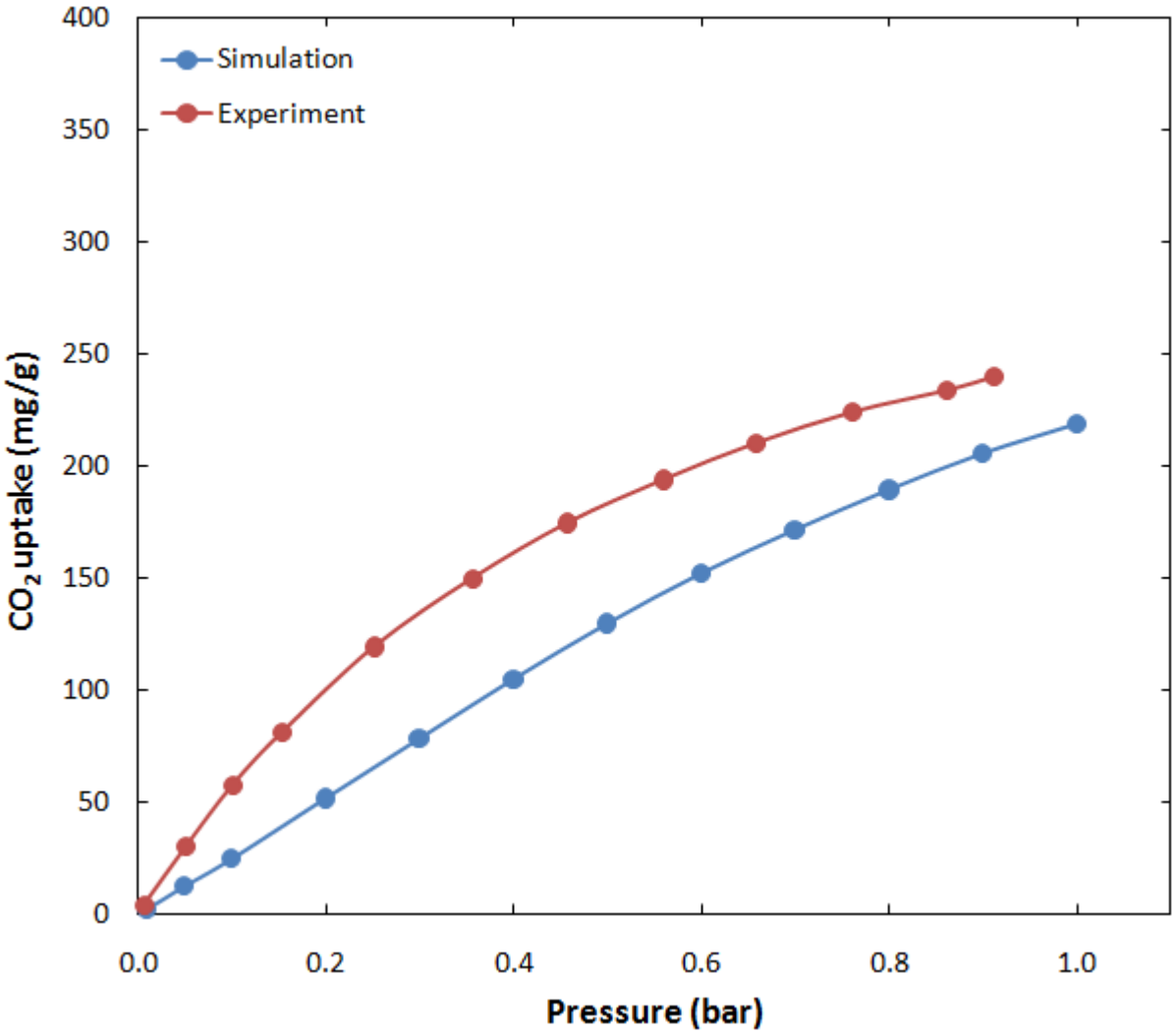

Figure S13. Comparison of simulated and experimental CO_2 adsorption isotherms in Zn\DOBDC at 296 K. Lines are drawn to guide the eye.

4.7. Ni\DOBDC

Partial atomic charges

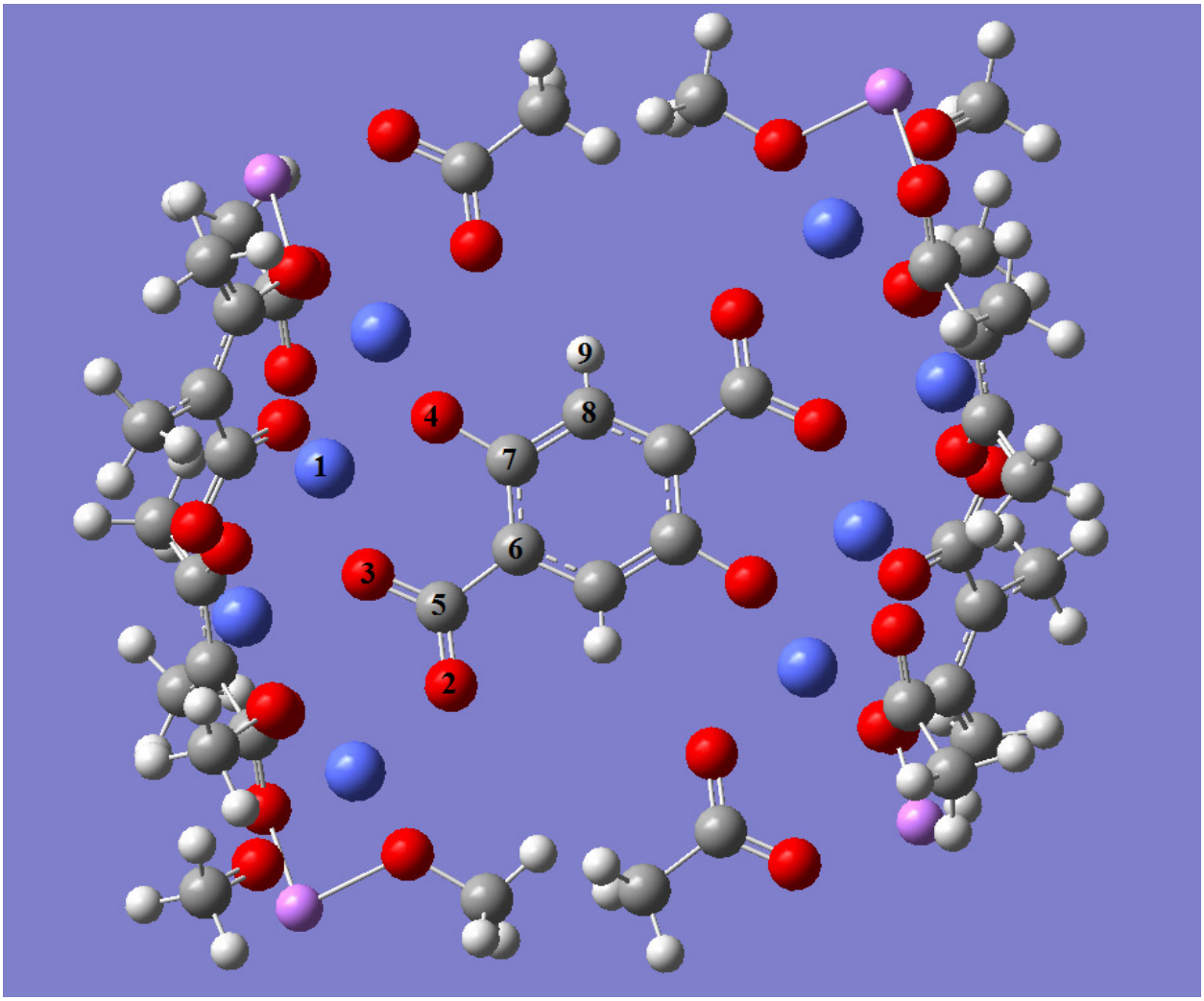

Figure S14. Cluster ($Ni_8C_{42}O_{32}H_{56}Li_4$) used for deriving partial charges on Ni\DOBDC atoms.

Table S16. Partial atomic charges for Ni\DOBDC atoms.

Atom no	1	2	3	4	5	6
Charge (e)	1.100 (Ni)	-0.677 (O)	-0.623 (O)	-0.679 (O)	0.789 (C)	-0.239 (C)
Atom no	**7**	**8**	**9**			
Charge (e)	0.358 (C)	-0.201 (C)	0.172(H)			

Table S17. GCMC simulation details for Ni\DOBDC.

Number of unit cells	Cut-off distance (Å)	Temperature (K)	Coordinates
2x2x4 = 16	12.8	298	Dietzel et al. 2006[7]

Experimental details

Ni\DOBDC (CPO-27-Ni) $Ni_2(DOBDC)(solv)_2(H_2O)_2$ was synthesized and washed according to the literature procedure.[7] The dirty mustard yellow powder was then dried at 100 °C in a furnace with flowing nitrogen for at least 4 hours. Before gas adsorption analysis, Ni\DOBDC was heated to 150 °C under dynamic vacuum for 16 hours. CO_2 adsorption data for Ni\DOBDC were collected according to the procedure described in section 3. For Figures 1 and 2 in the main text, experimental CO_2 data at 0.1 bar, 0.5 bar, and 1 bar were estimated by interpolation or extrapolation of the experimental data points.

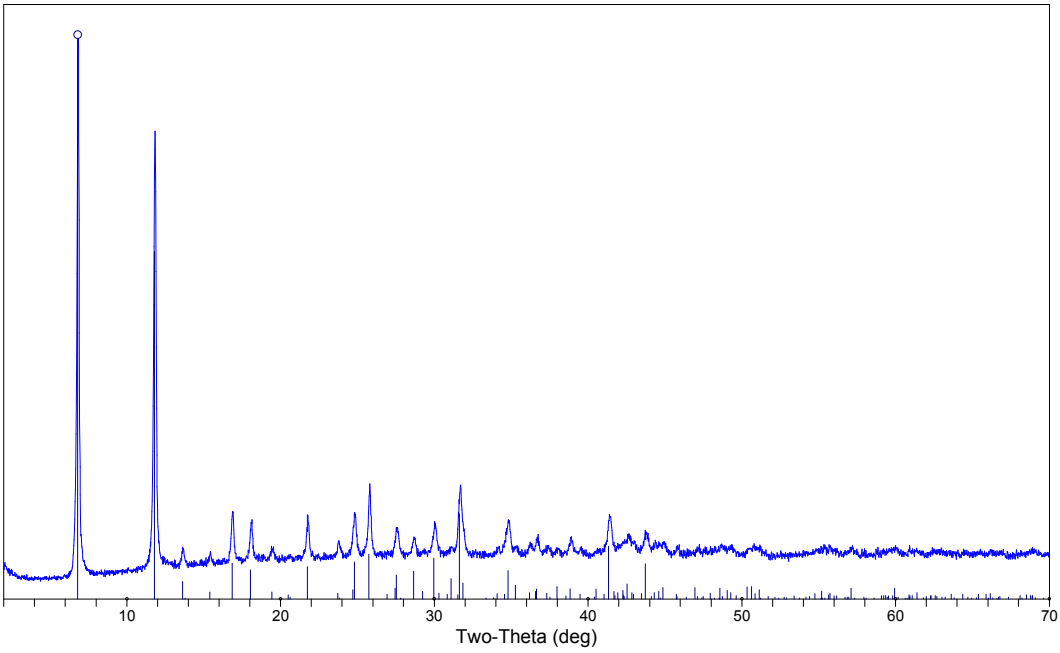

Figure S15. Powder x-ray diffraction (XRD) pattern for Ni\DOBDC. Sticks represent simulated powder patterns from data reported in the literature.

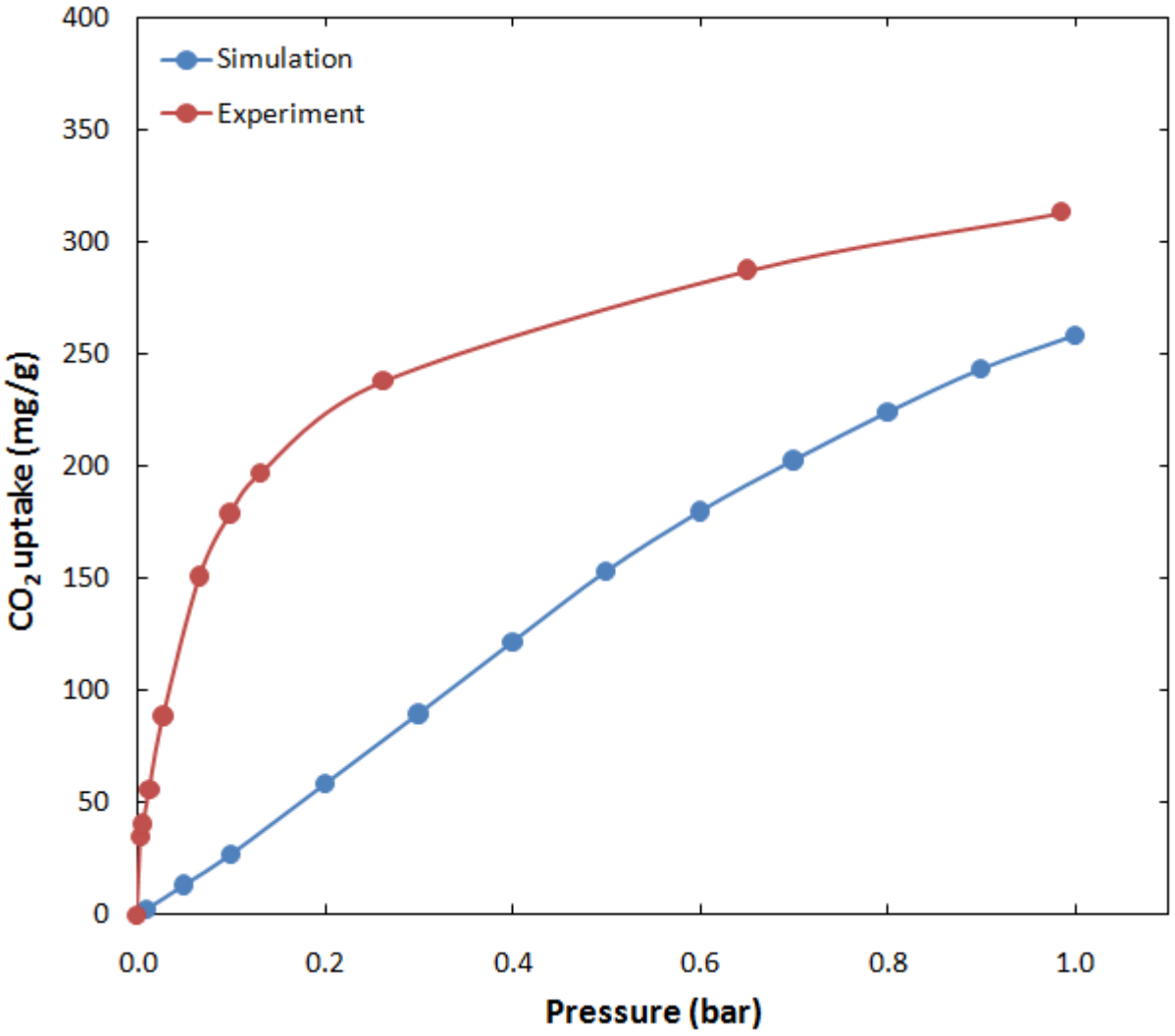

Figure S16. Comparison of simulated and experimental CO_2 adsorption isotherms in Ni\DOBDC at 298 K. Lines are drawn to guide the eye.

4.8. Co\DOBDC

Partial atomic charges

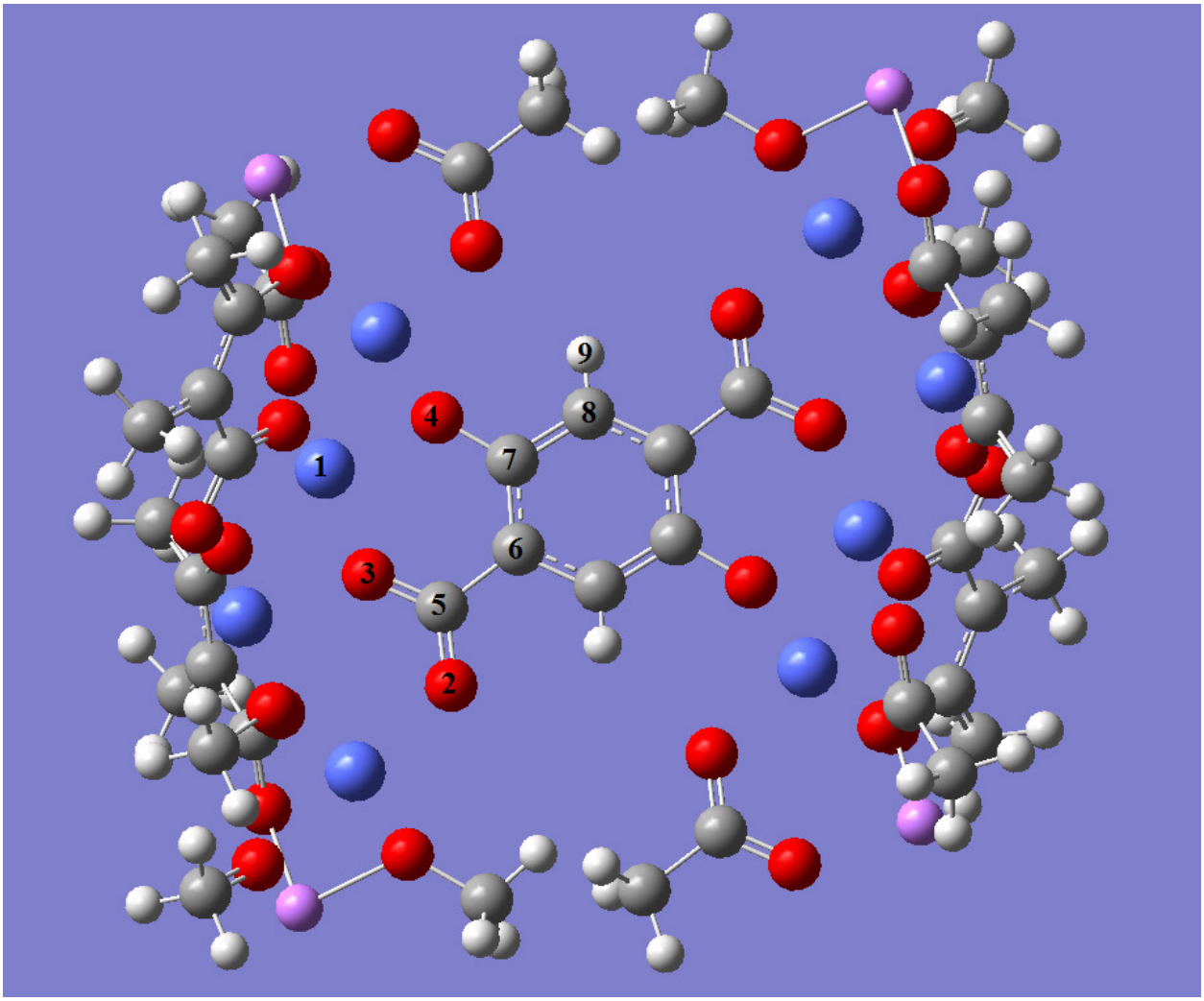

Figure S17. Cluster ($Co_8C_{42}O_{32}H_{56}Li_4$) used for deriving partial charges on Co\DOBDC atoms.

Table S18. Partial atomic charges for Co\DOBDC atoms.

Atom no	**1**	**2**	**3**	**4**	**5**	**6**
Charge (e)	1.139 (Co)	-0.684 (O)	-0.645 (O)	-0.731 (O)	0.832 (C)	-0.292 (C)
Atom no	**7**	**8**	**9**			
Charge (e)	0.315 (C)	-0.110 (C)	0.176 (H)			

Table S19. GCMC simulation details for Co\DOBDC.

Number of unit cells	**Cut-off distance (Å)**	**Temperature (K)**	**Coordinates**
2x2x4 = 16	12.8	298	Dietzel et al. 2005[8]

Experimental details

Co\DOBDC (CPO-27-Co) $Co_2(DOBDC)(solv)_2(H_2O)_2$ was synthesized and washed according to the literature procedure.[8] The red-orange powder was then dried at 100 °C in a furnace with flowing nitrogen for at least 4 hours. Before gas adsorption analysis, Co\DOBDC was heated to 170 °C under dynamic vacuum for 16 hours. CO_2 adsorption data for Co\DOBDC were collected according to the procedure described in section 3. For Figure Figures 1 and 2 in the main text, experimental CO_2 data at 0.1 bar, 0.5 bar, and 1 bar were estimated by interpolation or extrapolation of the experimental data points.

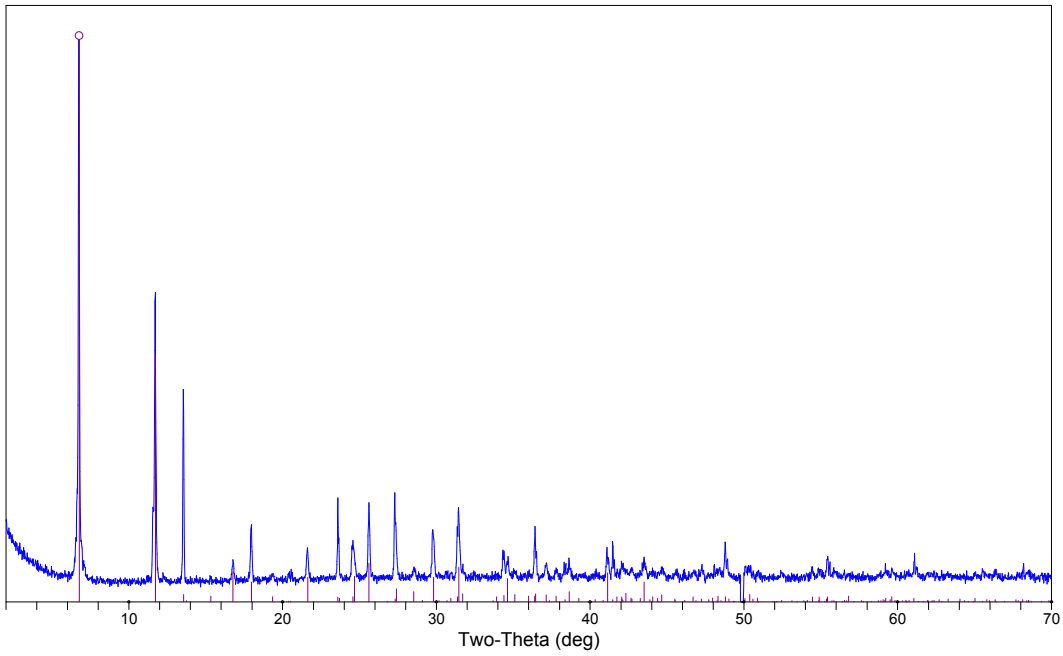

Figure S18. Powder x-ray diffraction (XRD) pattern for Co\DOBDC. Sticks represent simulated powder patterns from data reported in the literature.

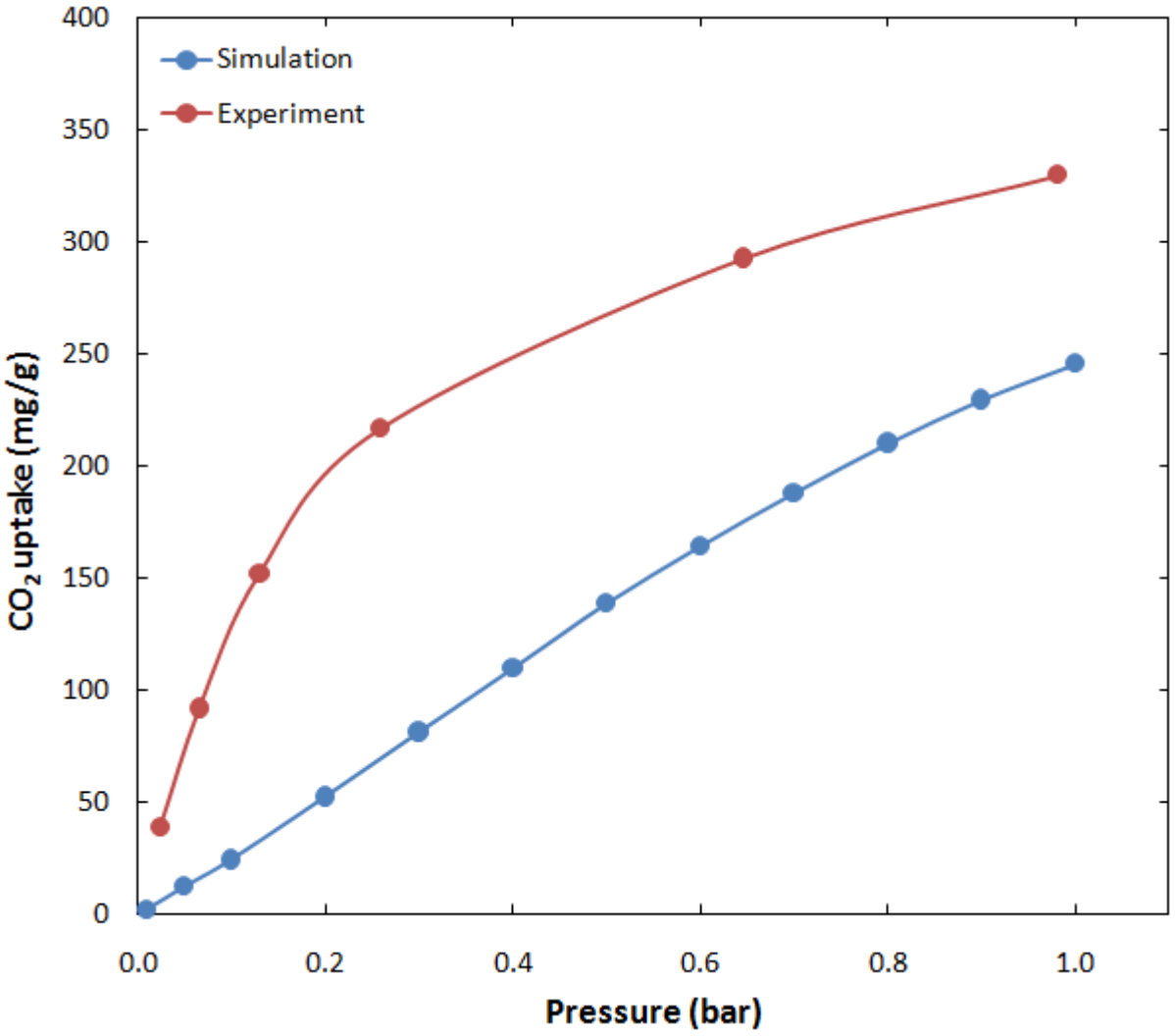

Figure S19. Comparison of simulated and experimental CO_2 adsorption isotherms in Co\DOBDC at 298 K. Lines are drawn to guide the eye.

4.9. Mg\DOBDC

Partial atomic charges

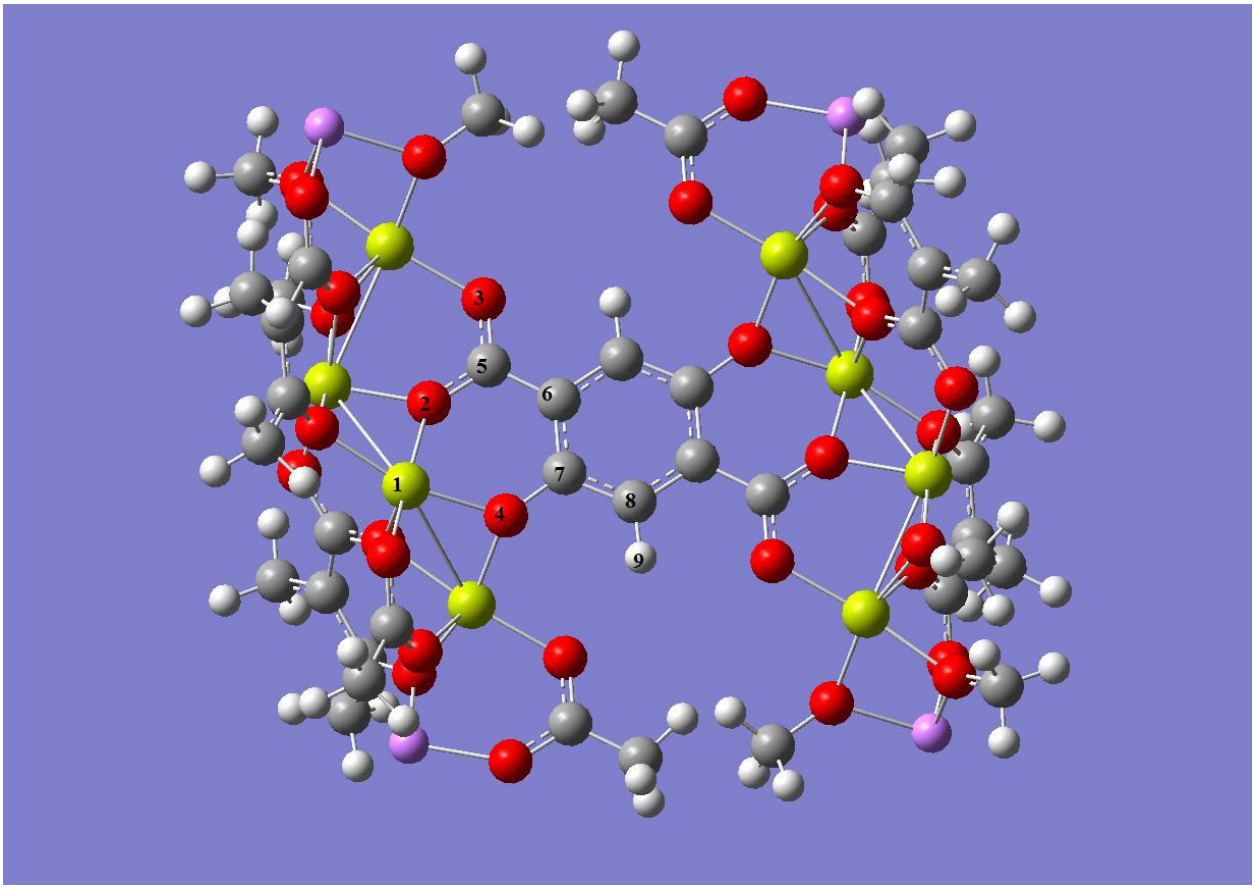

Figure S20. Cluster ($Mg_8C_{42}O_{32}H_{56}Li_4$) used for deriving partial charges on Mg\DOBDC

Table S20. Partial atomic charges for Mg\DOBDC atoms.

Atom no	**1**	**2**	**3**	**4**	**5**	**6**
Charge (e)	1.458 (Mg)	-0.909 (O)	-0.714 (O)	-0.784 (O)	0.8 (C)	-0.26 (C)
Atom no	**7**	**8**	**9**			
Charge (e)	0.492 (C)	-0.280 (C)	0.197 (H)			

Table S21. GCMC simulation details for Mg\DOBDC.

Number of unit cells	**Cut-off distance (Å)**	**Temperature (K)**	**Coordinates**
2x2x4 = 16	12.8	298	DFT optimization

DFT optimization details

Coordinates for Mg\DOBDC were obtained by replacing the zinc atoms of Zn\DOBDC with magnesium and optimizing the whole unit cell with VASP[32-35] software using the LDA[36] functional and ultrasoft psuedopotentials.[37,38]

Experimental details

Mg\DOBDC (Mg/DOBDC) samples were provided by Professor Adam Matzger at the University of Michigan. Synthesis and characterization details for Mg\DOBDC can be found in the work of Caskey et al.[9] CO_2 adsorption data for Mg\DOBDC were collected according to the procedure described in section 3. For Figures 1 and 2 in the main text, experimental CO_2 data at 0.1 bar, 0.5 bar, and 1 bar were estimated by interpolation or extrapolation of the experimental data points.

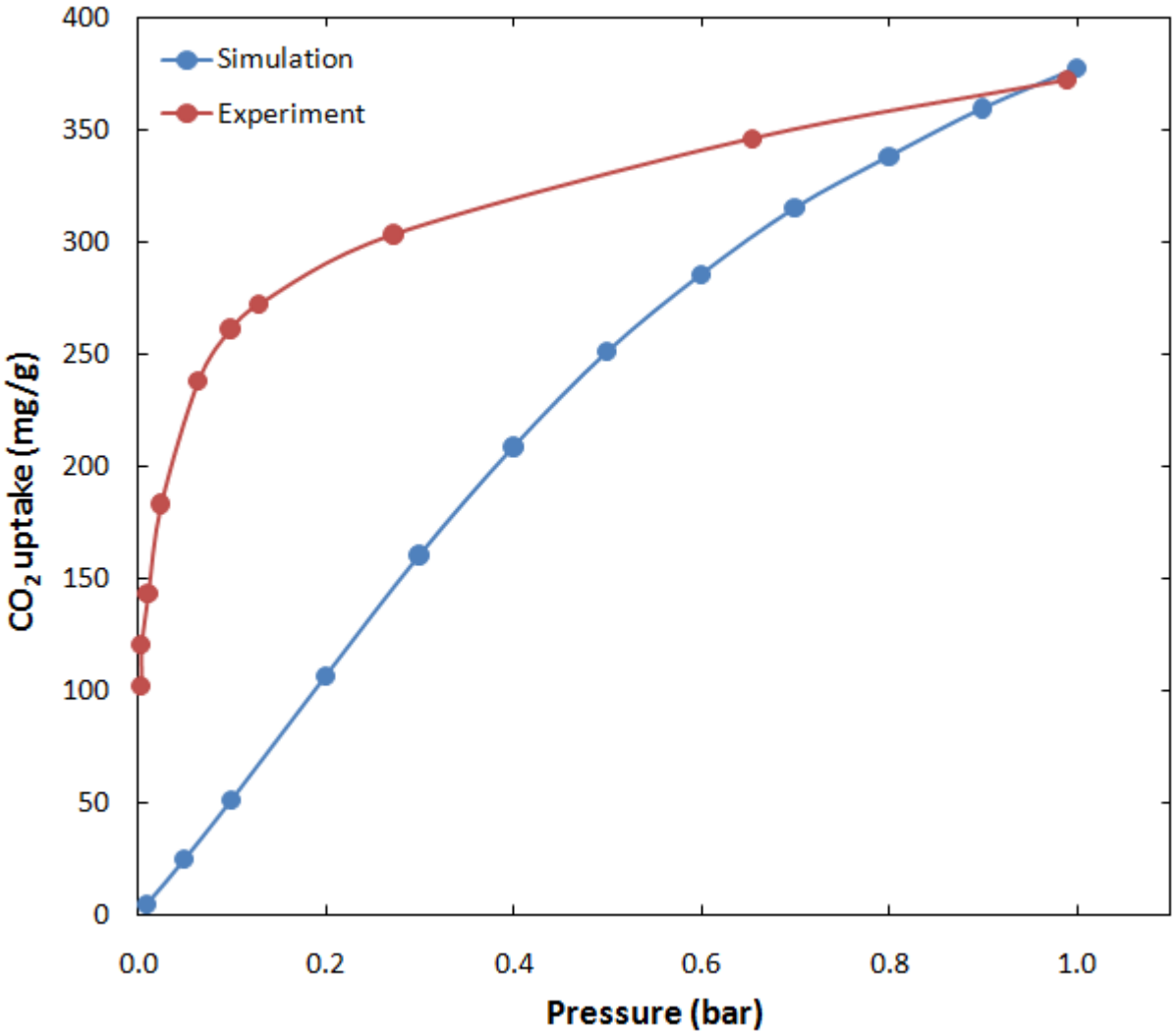

Figure S21. Comparison of simulated and experimental CO_2 adsorption isotherms in Mg\DOBDC at 298 K. Lines are drawn to guide the eye.

4.10. ZIF-8

Partial atomic charges

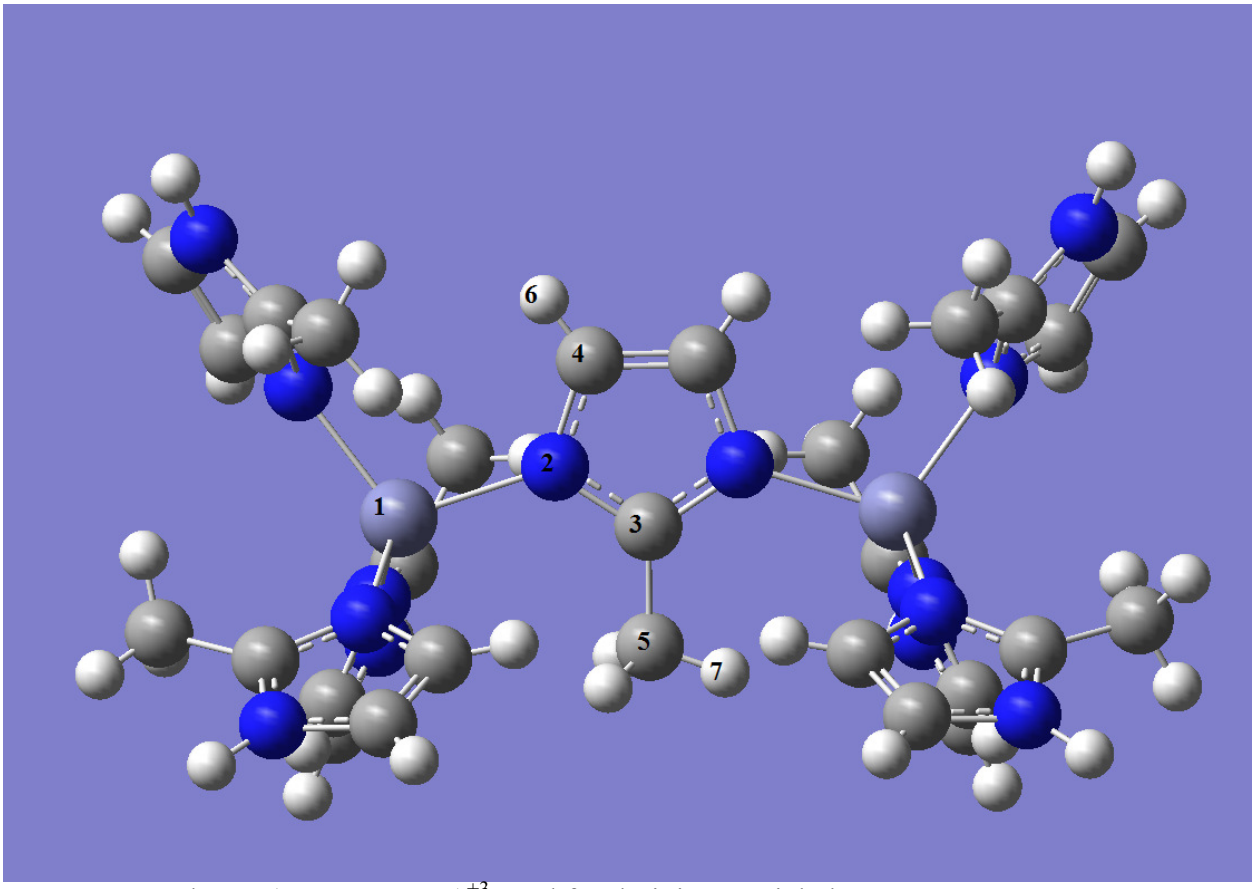

Figure S22. Cluster $(Zn_2C_{28}N_{14}H_{35})^{+3}$ used for deriving partial charges on ZIF-8 atoms.

Table S22. Partial atomic charges for ZIF-8 atoms.

Atom no	1	2	3	4	5	6	7
Charge (e)	0.808 (Zn)	-0.407 (N)	0.461 (C)	-0.134 (C)	-0.455 (C)	0.153 (H)	0.122 (H)

Table S23. GCMC simulation details for ZIF-8.

Number of unit cells	Cut-off distance (Å)	Temperature (K)	Coordinates
2x2x2 = 8	12.8	298	Park et al. 2006[10]

Experimental details

ZIF-8, $Zn(MeIM)_2 \cdot (DMF) \cdot (H_2O)_3$ was synthesized, purified by density separation, methanol activated and dried according to the literature procedure.[10] Before gas adsorption analysis, ZIF-8 was heated to 300 °C under dynamic vacuum for 18 hours. CO_2 adsorption data for ZIF-8 were collected according to the procedure described in section 3. For Figures 1 and 2 in the main text, experimental CO_2 data at 0.1 bar, 0.5 bar, and 1 bar were estimated by interpolation or extrapolation of the experimental data points.

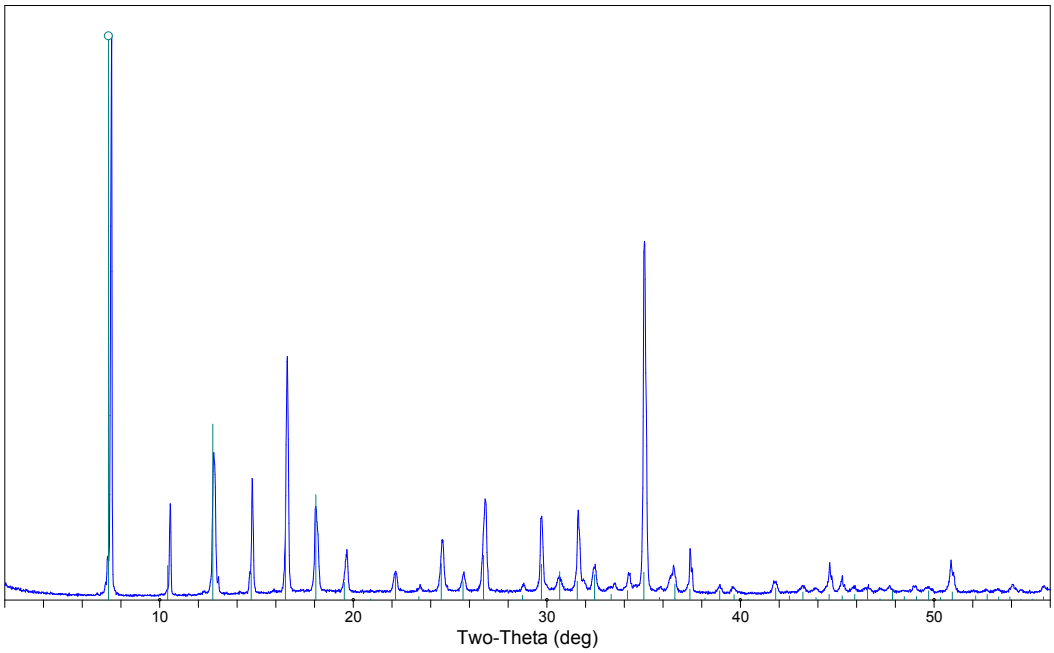

Figure S23. Powder x-ray diffraction (XRD) pattern for ZIF-8. Sticks represent simulated powder patterns from data reported in the literature.

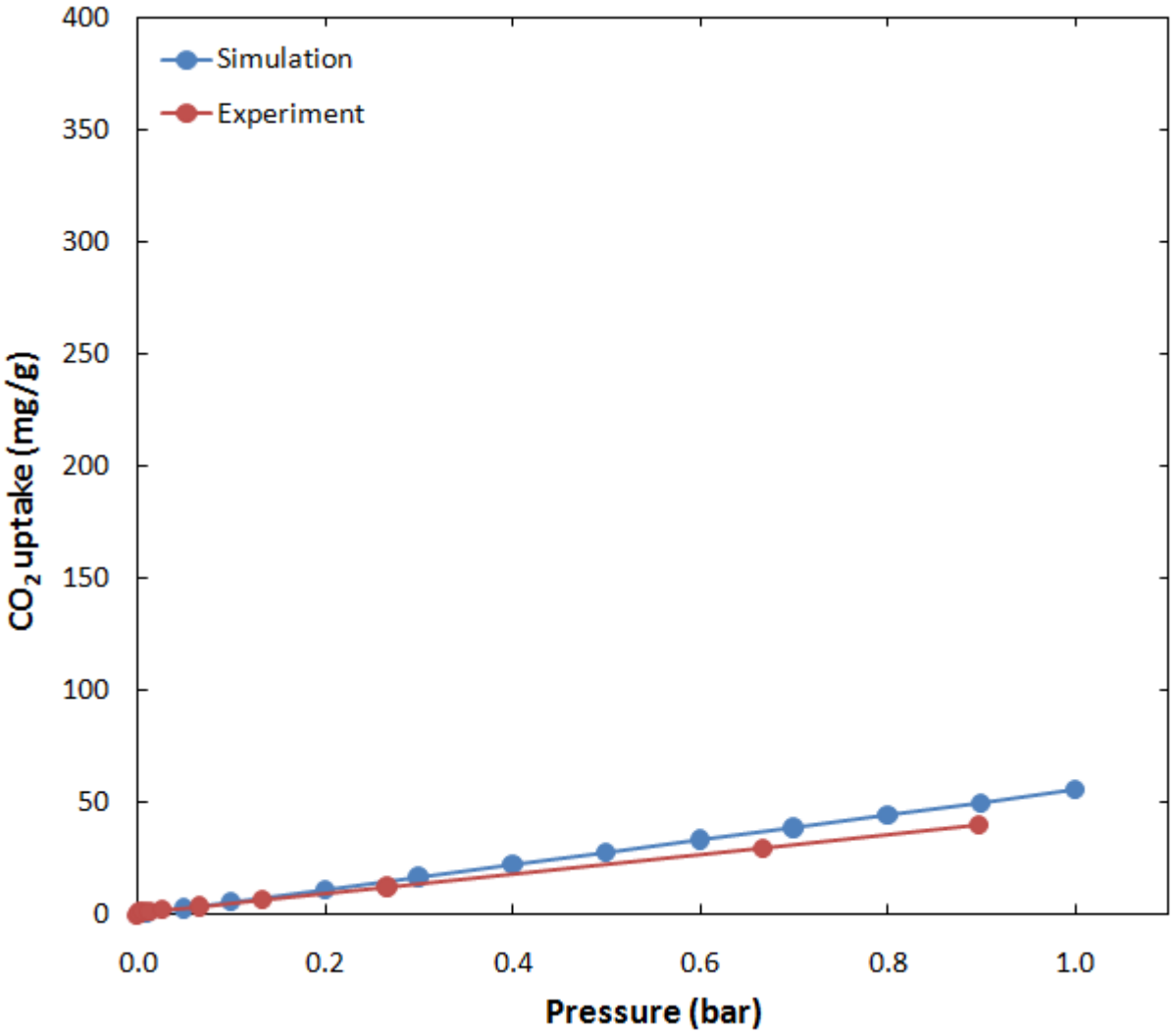

Figure S24. Comparison of simulated and experimental CO_2 adsorption isotherms in ZIF-8 at 298 K. Lines are drawn to guide the eye.

4.11. MIL-47

Partial atomic charges

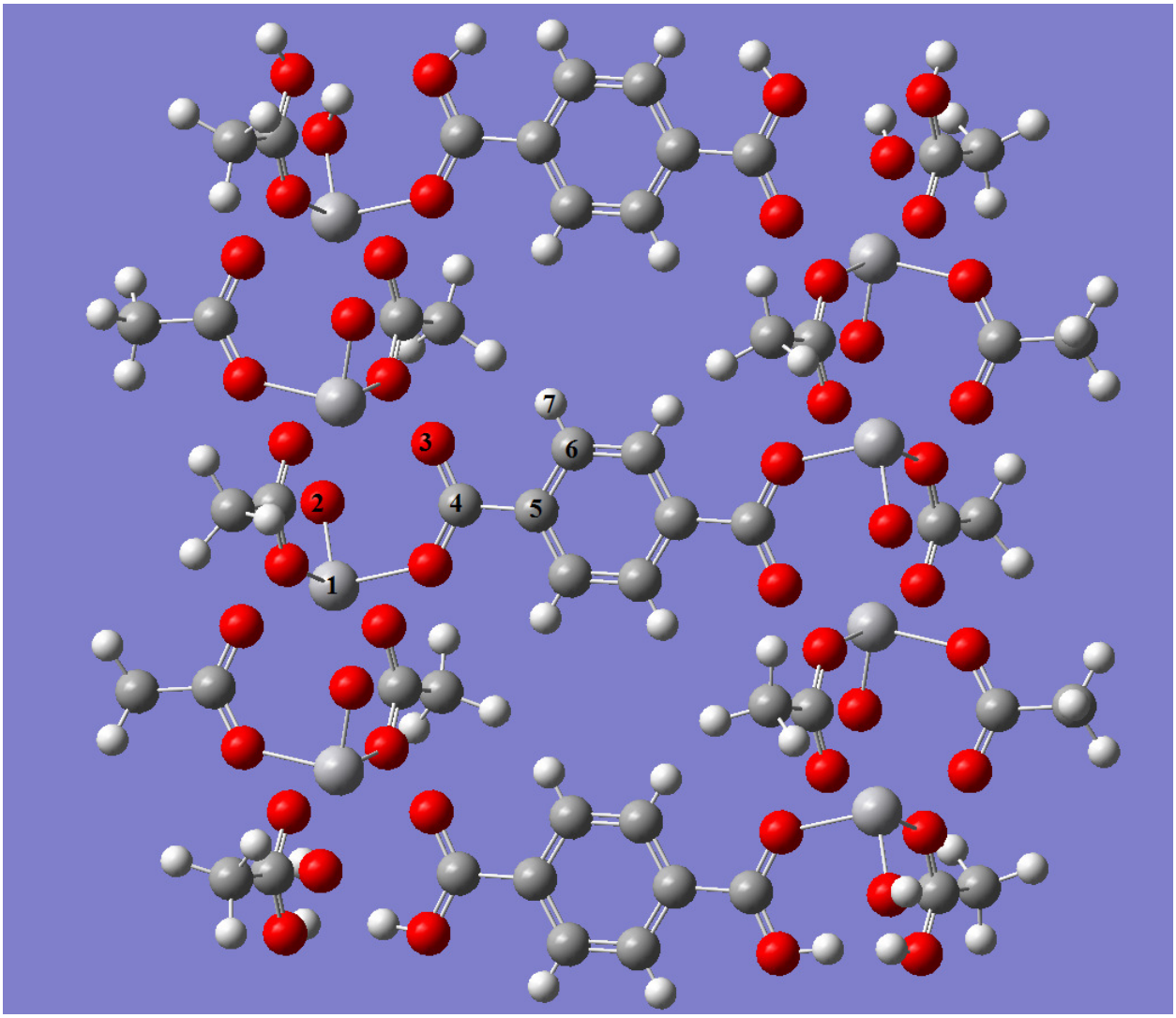

Figure S25. Cluster ($V_8C_{52}O_{50}H_{66}$) used for deriving partial charges on MIL-47 atoms.

Table S24. Partial atomic charges for MIL-47 atoms.

Atom no	1	2	3	4	5	6	7
Charge (e)	1.77 (V)	-0.662 (O)	-0.611 (O)	0.644 (C)	0.32 (C)	-0.153 (C)	0.149 (H)

Table S25. GCMC simulation details for MIL-47.

Number of unit cells	Cut-off distance (Å)	Temperature (K)	Coordinates
4x2x2 = 16	12.8	298	Barthelet et al. 2002[11]

Experimental details

MIL-47, $V^{IV}O$(BDC), was hydrothermally synthesized according to the literature procedure[11] with VCl_3 and terephthalic acid in water, collected by filtration, and air dried. The powder was then calcined in air at 275 °C for 21.5 hours to remove uncoordinated terephthalic acid within the pores. Before gas adsorption analysis, MIL-47 was heated to 150 °C under dynamic vacuum for 18 hours. CO_2 adsorption data for MIL-47 were collected according to the procedure described in section 3. For Figures 1 and 2 in the main text, experimental CO_2 data at 0.1 bar, 0.5 bar, and 1 bar were estimated by interpolation or extrapolation of the experimental data points.

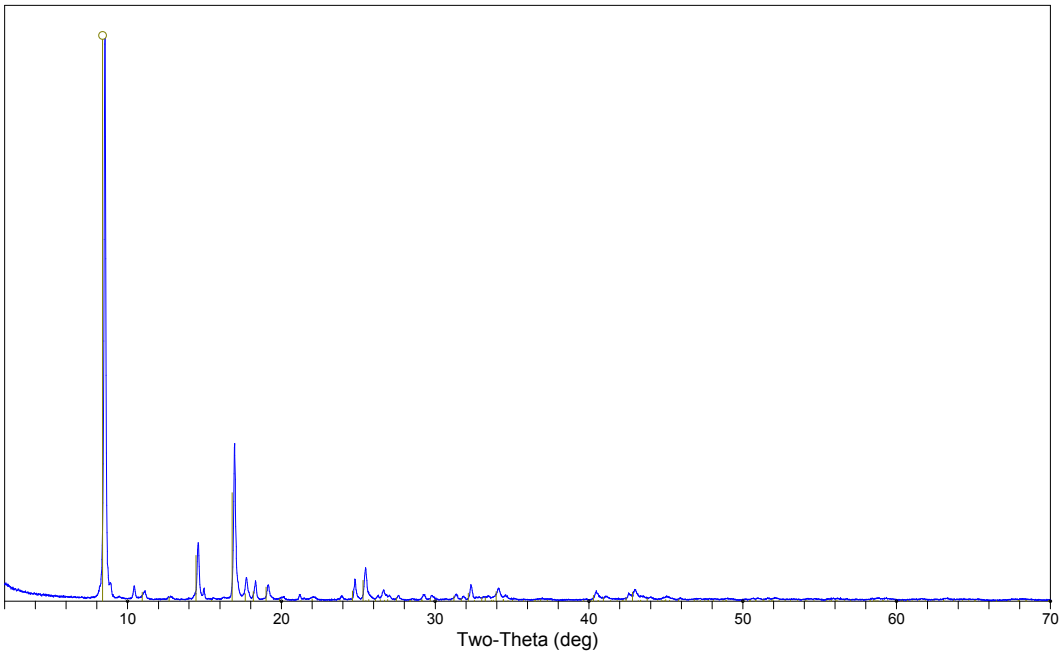

Figure S26. Powder x-ray diffraction (XRD) pattern for MIL-47. Sticks represent simulated powder patterns from data reported in the literature.

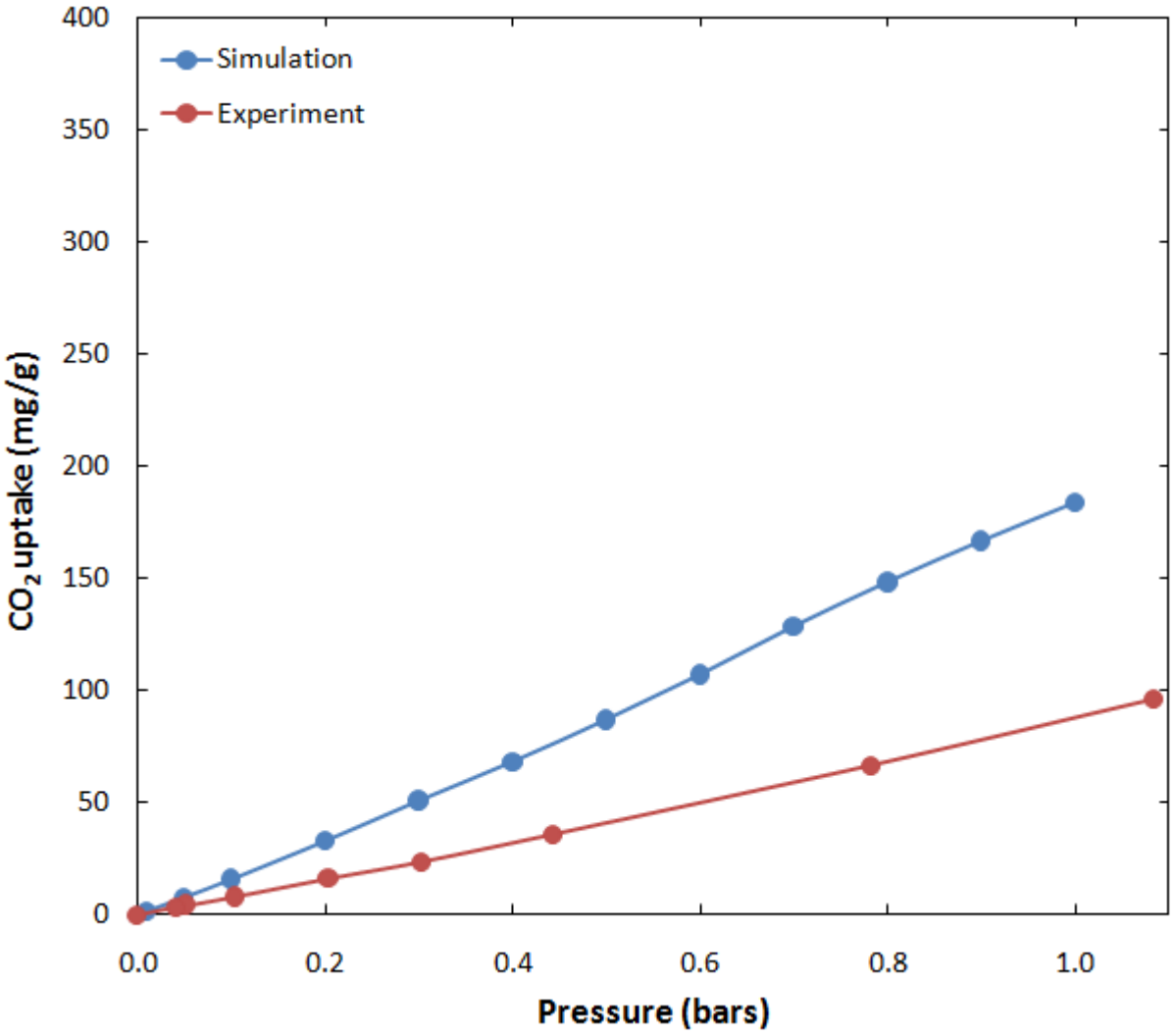

Figure S27. Comparison of simulated and experimental CO_2 adsorption isotherms in MIL-47 at 298 K. Lines are drawn to guide the eye.

4.12. UMCM-1

Partial atomic charges

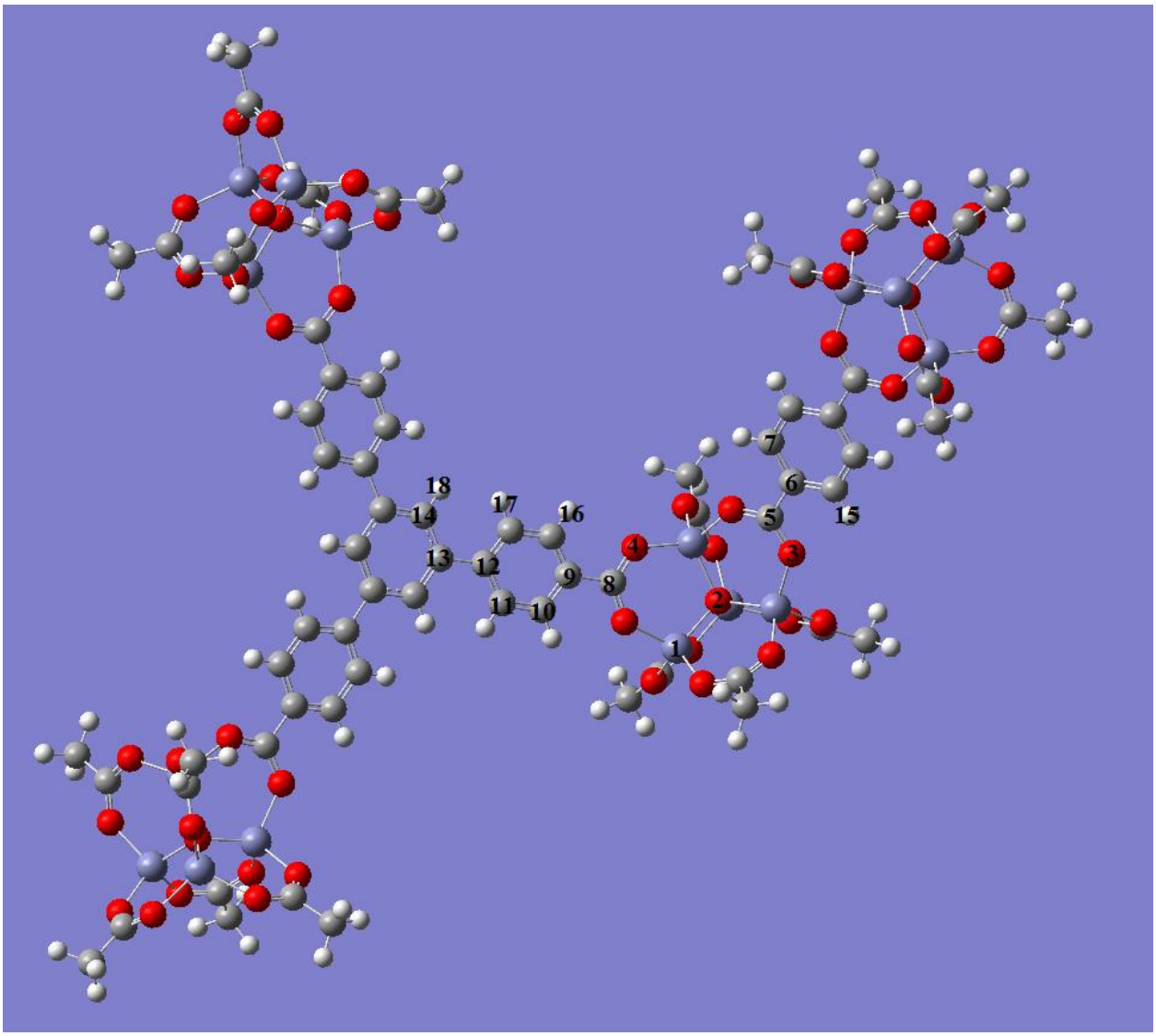

Figure S28. Cluster ($Zn_{16}C_{73}O_{52}H_{76}$) used for deriving partial charges on UMCM-1 atoms.

Table S26. Partial atomic charges for UMCM-1 atoms.

Atom no	**1**	**2**	**3**	**4**	**5**	**6**
Charge (e)	1.394 (Zn)	-1.626 (O)	-0.699 (O)	-0.673 (O)	0.661 (C)	0.064 (C)
Atom no	**7**	**8**	**9**	**10**	**11**	**12**
Charge (e)	-0.165 (C)	0.607 (C)	0.148 (C)	-0.202 (C)	-0.130 (C)	0.062 (C)
Atom no	**13**	**14**	**15**	**16**	**17**	**18**
Charge (e)	0.082 (C)	-0.24 (C)	0.15 (H)	0.131 (H)	0.101 (H)	0.155 (H)

Table S27. GCMC simulation details for UMCM-1.

Number of unit cells	Cut-off distance (Å)	Temperature (K)	Coordinates
1x1x2 = 2	12.8	298	Koh et al. 2008[12]

Experimental details

UMCM-1, $Zn_4O(BDC)(BTB)_{4/3}$, was synthesized and solvent exchanged according to the literature procedure.[12] Before gas adsorption analysis, UMCM-1 was charged into a sample cell and dried under vacuum (< 0.1 millitorr) at room temperature for 2 hours. CO_2 adsorption data for UMCM-1 were collected according to the procedure described in section 3. For Figures 1 and 2 in the main text, experimental CO_2 data at 0.1 bar, 0.5 bar, and 1 bar were estimated by interpolation or extrapolation of the experimental data points.

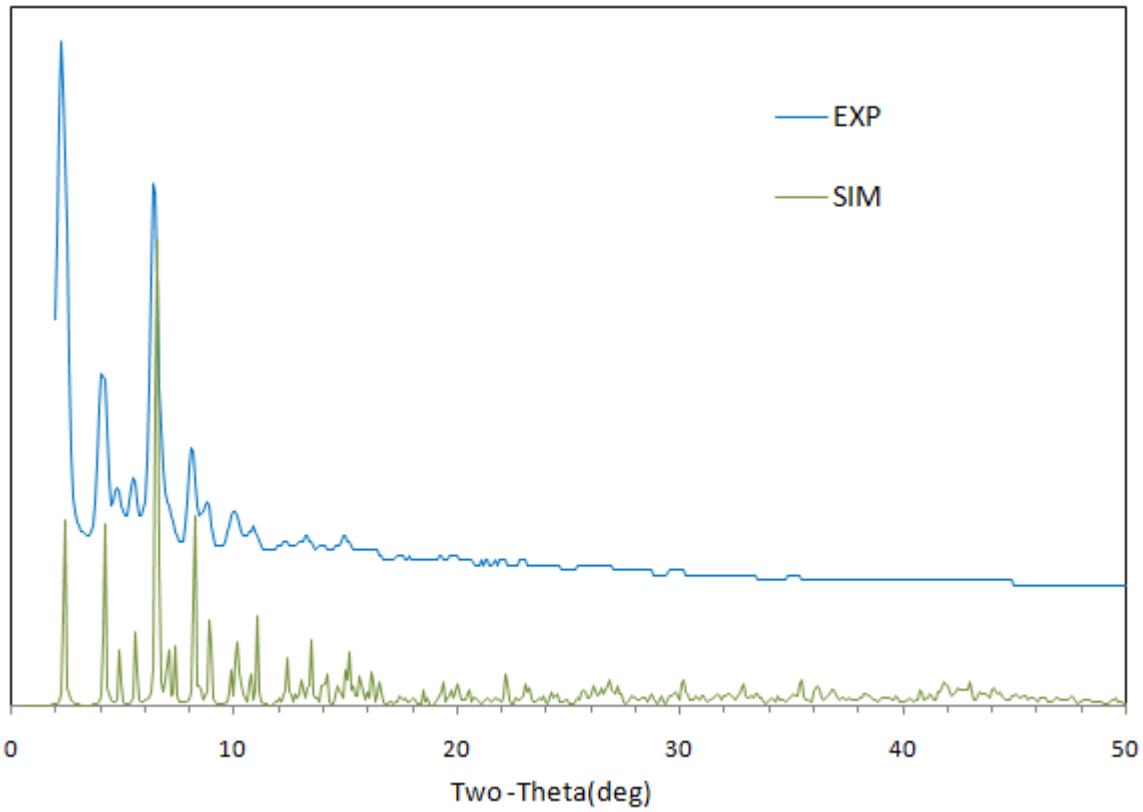

Figure S29. Powder x-ray diffraction (XRD) pattern for UMCM-1.

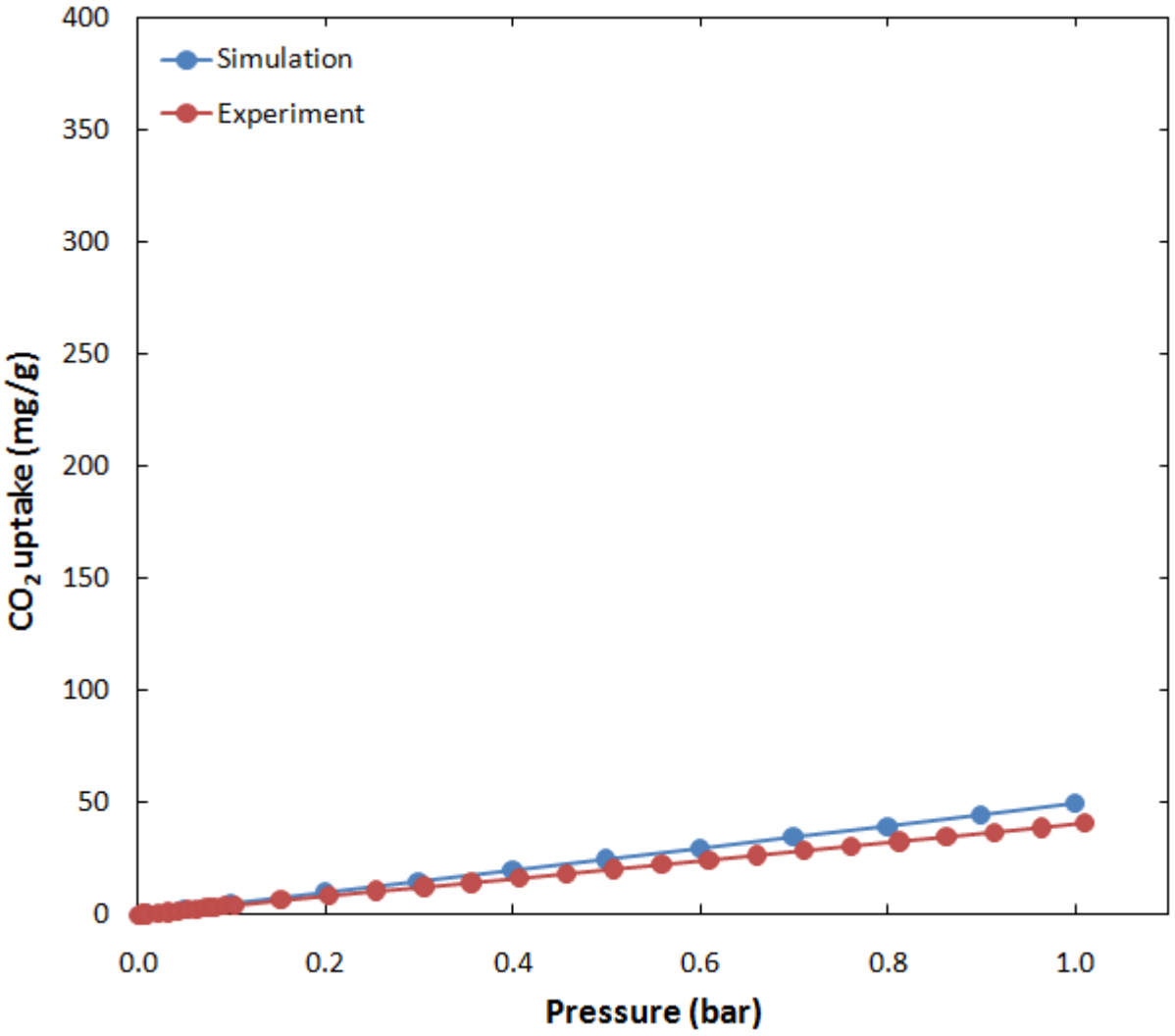

Figure S30. Comparison of simulated and experimental CO_2 adsorption isotherms in UMCM-1 at 298 K. Lines are drawn to guide the eye.

4.13. UMCM-150

Partial atomic charges

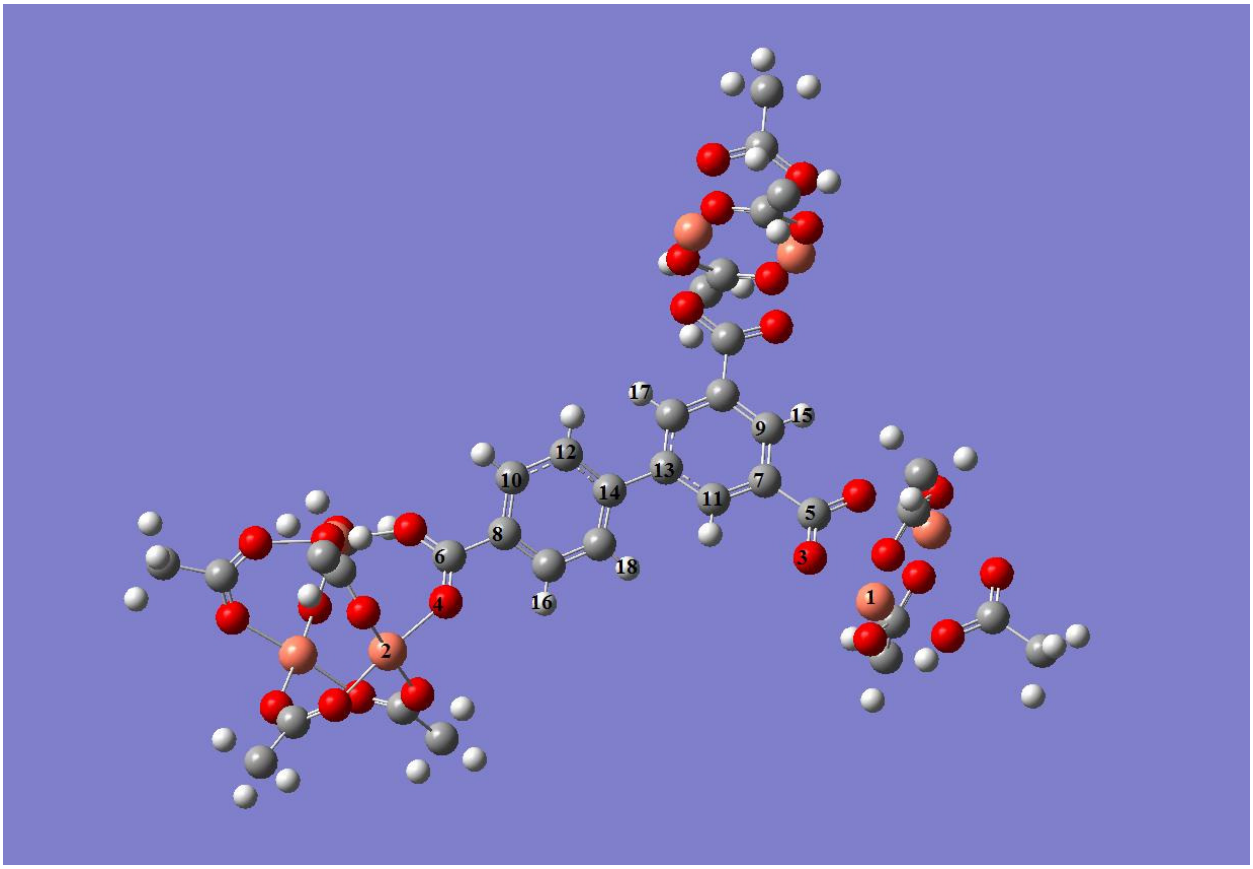

Figure S31. Cluster ($Cu_7C_{37}O_{28}H_{40}$) used for deriving partial charges on UMCM-150 atoms.

Table S28. Partial atomic charges for UMCM-150 atoms.

Atom no	**1**	**2**	**3**	**4**	**5**	**6**
Charge (e)	1.116 (Cu)	0.836 (Cu)	-0.643 (O)	-0.515 (O)	0.709 (C)	0.647 (C)
Atom no	**7**	**8**	**9**	**10**	**11**	**12**
Charge (e)	-0.011 (C)	-0.017 (C)	-0.123 (C)	-0.124 (C)	-0.135 (C)	-0.159 (C)
Atom no	**13**	**14**	**15**	**16**	**17**	**18**
Charge (e)	0.027 (C)	0.067 (C)	0.130 (H)	0.115 (H)	0.136 (H)	0.137 (H)

Table S29. GCMC simulation details for UMCM-150.

Number of unit cells	**Cut-off distance (Å)**	**Temperature (K)**	**Coordinates**
2x2x1 = 4	12.8	298	Wong-Foy et al. 2007[13]

Experimental details

Experimental CO_2 adsorption data were taken from the work of Park et al. 2009.[14] For Figures 1 and 2 in the main text, experimental CO_2 data at 0.1 bar, 0.5 bar, and 1 bar were estimated by interpolation or extrapolation of the experimental data points.

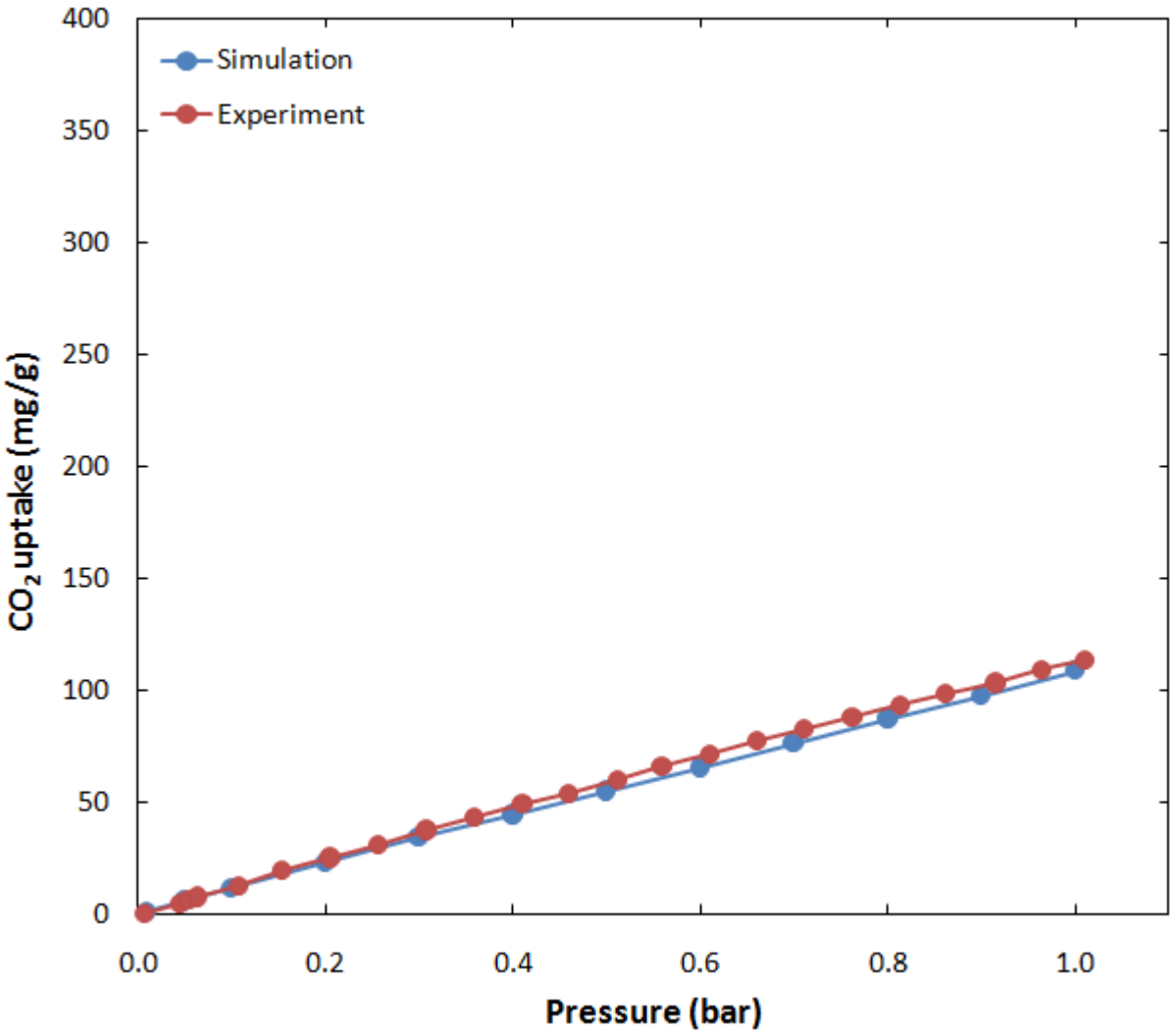

Figure S32. Comparison of simulated and experimental CO_2 adsorption isotherms in UMCM-150 at 298 K. Lines are drawn to guide the eye.

4.14. UMCM-150(N)$_2$

Partial atomic charges

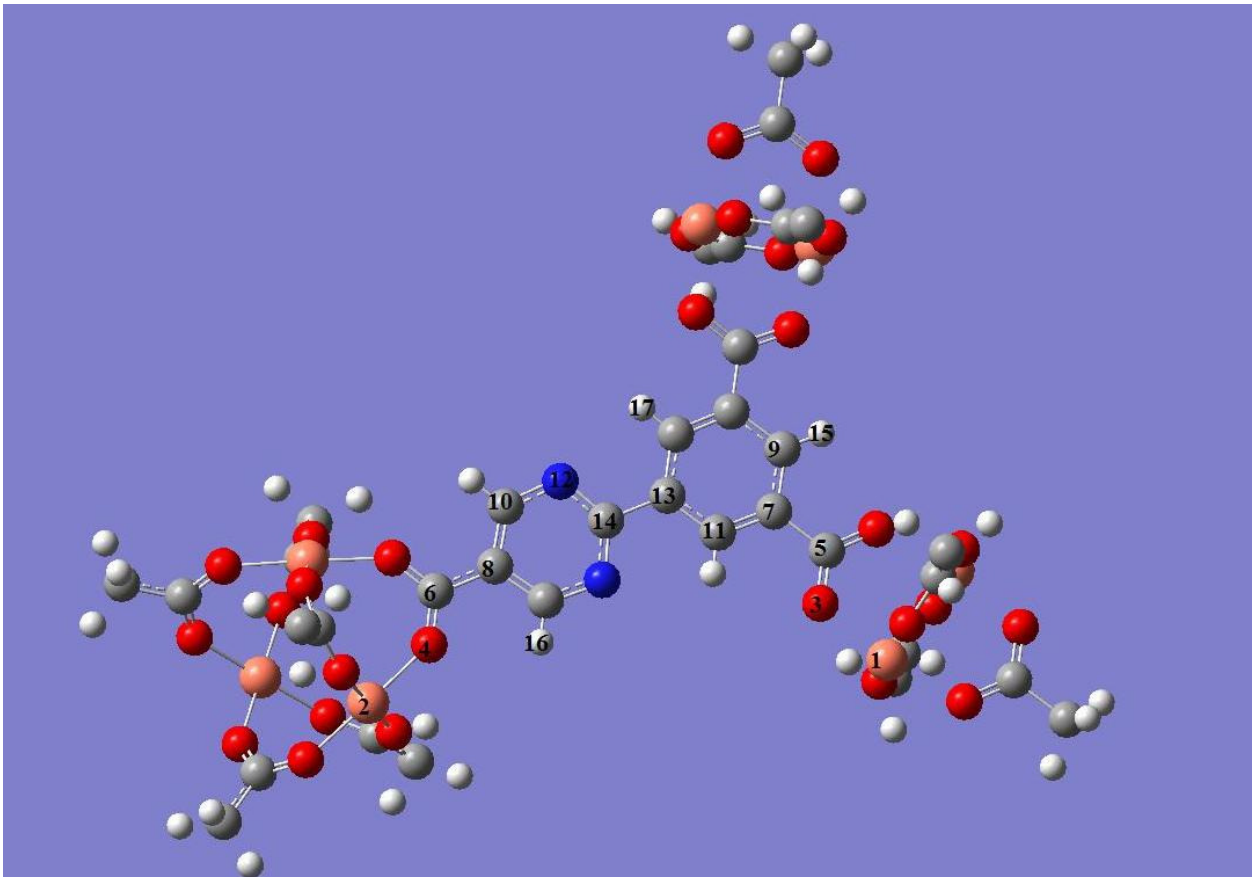

Figure S33. Cluster ($Cu_7C_{35}N_2O_{28}H_{38}$) used for deriving partial charges on UMCM-150(N)$_2$ atoms.

Table S30. Partial atomic charges for UMCM-150(N)$_2$ atoms.

Atom no	**1**	**2**	**3**	**4**	**5**	**6**
Charge (e)	1.136 (Cu)	0.946 (Cu)	-0.651(O)	-0.547 (O)	0.739 (C)	0.698 (C)
Atom no	**7**	**8**	**9**	**10**	**11**	**12**
Charge (e)	-0.104 (C)	-0.393 (C)	-0.065 (C)	0.432 (C)	0.077 (C)	-0.664 (N)
Atom no	**13**	**14**	**15**	**16**	**17**	
Charge (e)	-0.324 (C)	0.877 (C)	0.134 (H)	0.028 (H)	0.073 (H)	

Table S31. GCMC simulation details for UMCM-150(N)$_2$.

Number of unit cells	**Cut-off distance (Å)**	**Temperature (K)**	**Coordinates**
2x2x1 = 4	12.8	298	Park et al. 2009[14]

Experimental details

Experimental CO_2 adsorption data were taken from the work of Park et al. 2009.[14] For Figures 1 and 2 in the main text, experimental CO_2 data at 0.1 bar, 0.5 bar, and 1 bar were estimated by interpolation or extrapolation of the experimental data points.

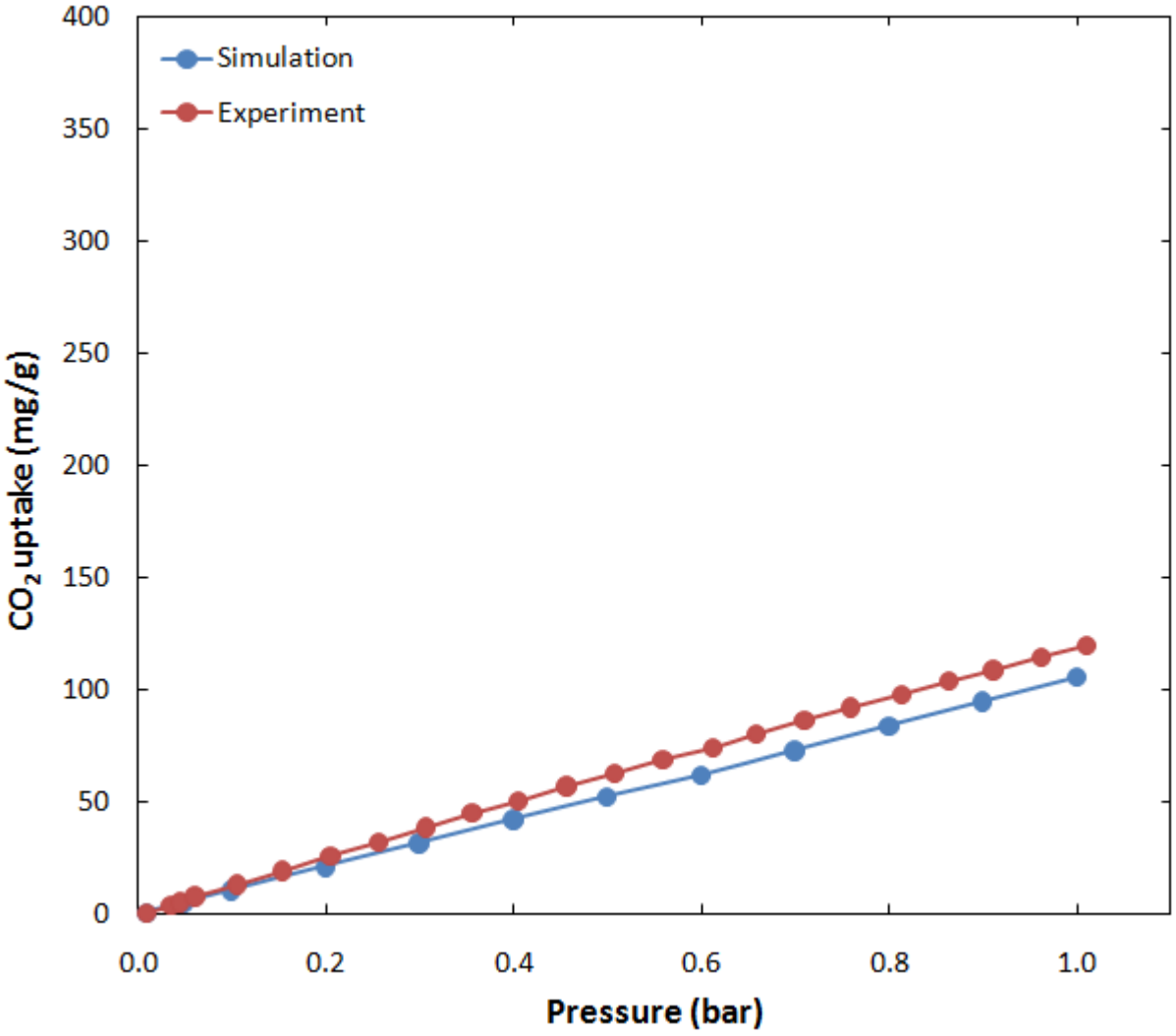

Figure S34. Comparison of simulated and experimental CO_2 adsorption isotherms in UMCM-150$(N)_2$ at 298 K. Lines are drawn to guide the eye.

5. Supplementary Results, Figures and Tables

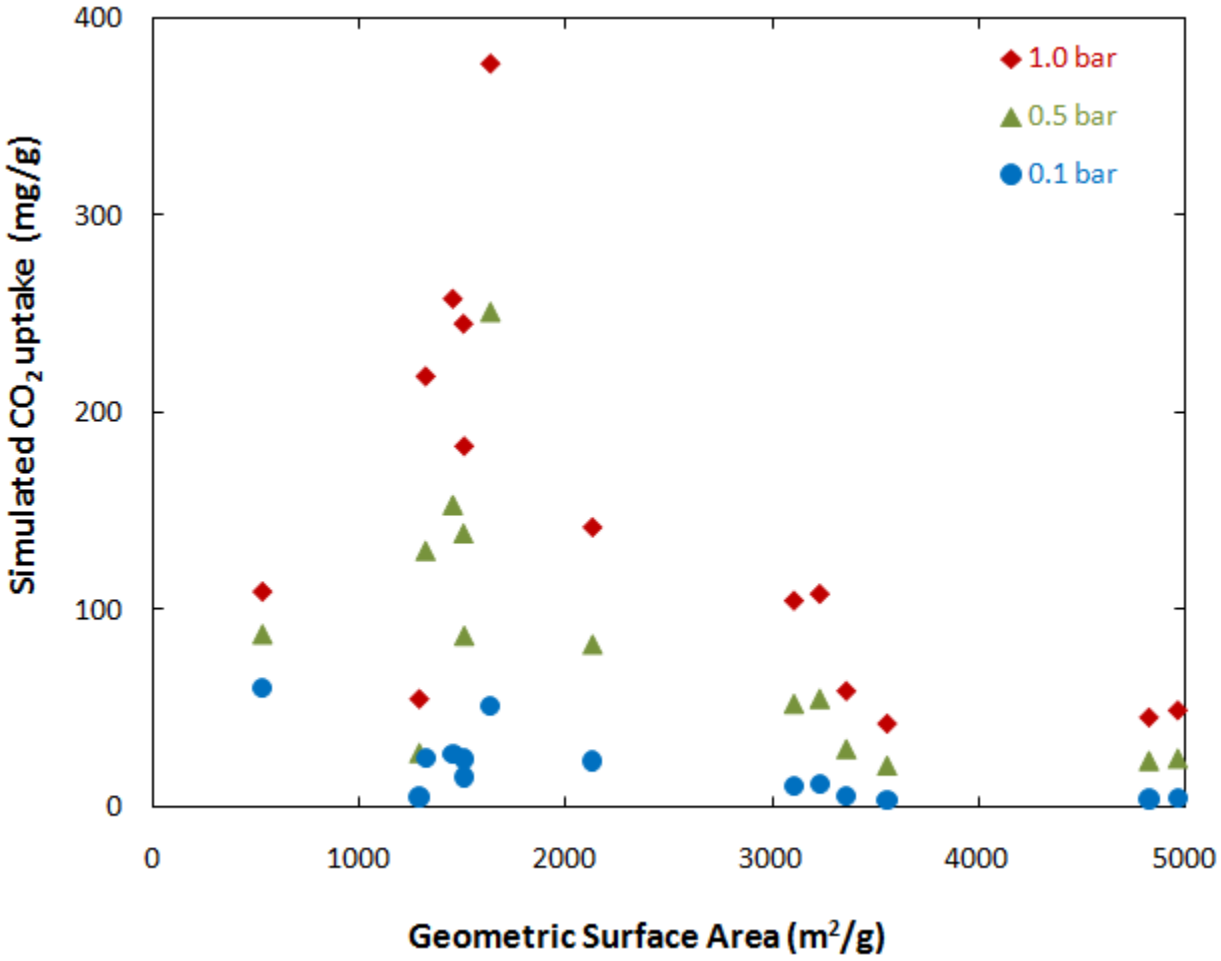

Figure S35. Geometric surface area and simulated CO_2 uptake in screened MOFs at 0.1 bar, 0.5 bar and 1 bar. Data were obtained at temperatures that ranged from 293 K to 298 K. See the relevant part for exact temperature for each MOF. No correlation is observed between CO_2 uptake and MOF surface area at these pressures.

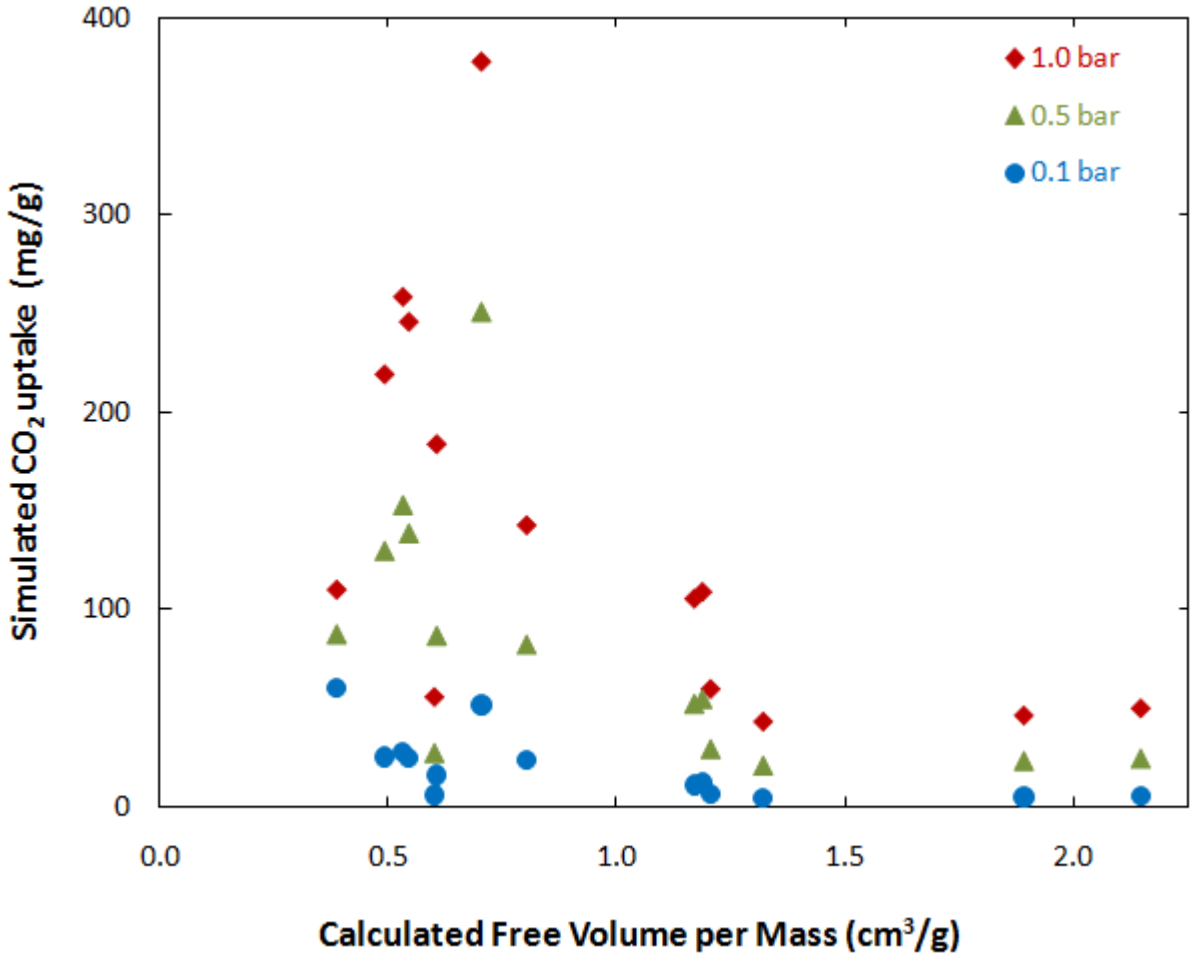

Figure S36. Geometric free volume and simulated CO_2 uptake in screened MOFs at 0.1 bar, 0.5 bar and 1 bar. Data were obtained at temperatures that ranged from 293 K to 298 K. See the relevant part for exact temperature for each MOF. No correlation is observed between CO_2 uptake and MOF free volume at these pressures.

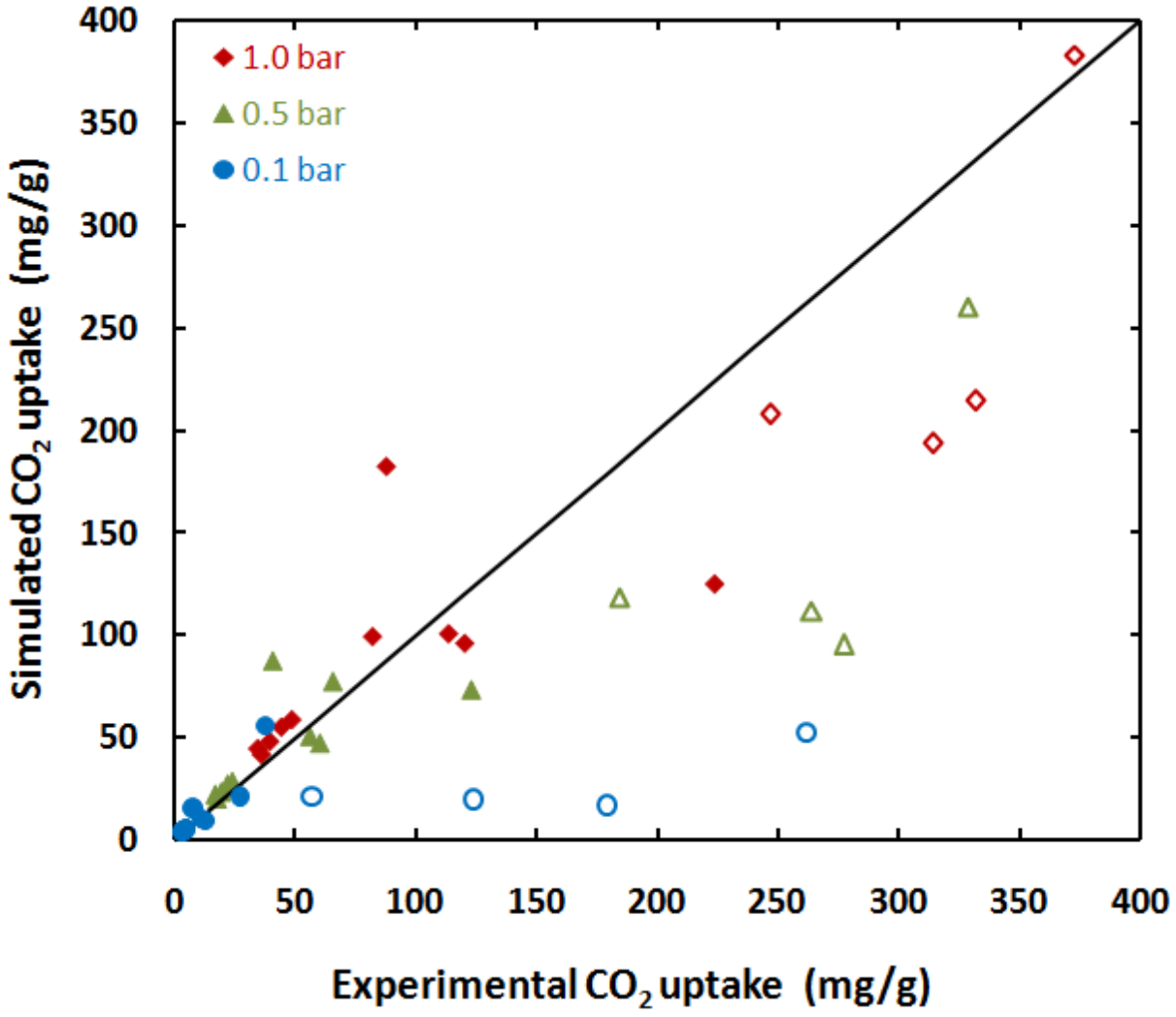

Figure S37. Comparison of simulated and experimental CO_2 uptake in screened MOFs at 0.1 bar, 0.5 bar and 1 bar. The simulated data in this figure were obtained by using partial charges derived from DFT calculations in which the PBEPBE functional was used. Data for M\DOBDC samples are shown in open symbols. If the M\DOBDC data at 0.1 bar (open blue circles) are excluded, the linear correlation coefficient R^2 = 0.79; with all data included, R^2 = 0.67. Data were obtained at temperatures that ranged from 293 K to 298 K. Full results from these simulations are not given in this manuscript; however, this figure provides a comparison with Figure 2 in the main text where partial charges were derived from using the B3LYP functional.

Table S32. Data used in Figure 2.*

	CO_2 uptake at 0.1 bar		CO_2 uptake at 0.5 bar		CO_2 uptake at 1 bar	
	Experiment (mg/g)	**Simulation (mg/g)**	**Experiment (mg/g)**	**Simulation (mg/g)**	**Experiment (mg/g)**	**Simulation (mg/g)**
HKUST-1 (295 K)	27.3	23.7	123.5	82.5	224.2	142.7
$Pd(2\text{-pymo})_2$ (293 K)	37.9	60.1	66.2	87.8	82.5	110.0
IRMOF-1	3.5	4.2	18.3	21.1	36.5	43.1
IRMOF-3	4.9	5.8	24.6	29.5	49.1	59.7
MOF-177	3.5	4.7	17.5	23.6	35.0	46.3
Zn\DOBDC (296 K)	57.4	24.9	184.5	130.0	246.9	219.2
Ni\DOBDC	179.1	27.2	277.6	153.3	314.5	258.5
Co\DOBDC	123.8	24.7	264.3	138.9	332.1	245.8
Mg\DOBDC	261.6	51.5	329.1	251.2	373.2	377.7
ZIF-8	5.3	5.5	22.6	27.6	44.7	55.6
MIL-47	7.8	15.7	41.3	87.0	88.2	183.8
UMCM-1	4.1	4.9	20.0	24.7	39.9	49.8
UMCM-150	11.3	11.8	56.7	55.0	114.0	108.9
$UMCM\text{-}150(N)_2$	12.9	10.8	60.8	52.5	120.7	105.5

*Unless otherwise noted all data were obtained at 298 K.

Table S33. Data used in Figure 3.*

	0.1 bar		0.5 bar		1 bar	
	Q_{st} (kJ/mol)	**CO_2 uptake (mg/g)**	**Q_{st} (kJ/mol)**	**CO_2 uptake (mg/g)**	**Q_{st} (kJ/mol)**	**CO_2 uptake (mg/g)**
HKUST-1 (295 K)	25.1	23.7	24.0	82.5	23.3	142.7
Pd(2-pymo)$_2$ (293 K)	48.6	60.1	45.3	87.8	43.1	110.0
IRMOF-1	15.8	4.2	15.8	21.1	15.9	43.1
IRMOF-3	17.3	5.8	17.3	29.5	17.4	59.7
MOF-177	15.7	4.7	15.7	23.6	15.7	46.3
Zn\DOBDC (296 K)	24.4	24.9	25.1	130.0	25.6	219.2
Ni\DOBDC	26.0	27.2	27.2	153.3	27.9	258.5
Co\DOBDC	25.4	24.7	26.4	138.9	27.1	245.8
Mg\DOBDC	26.7	51.5	27.9	251.2	28.4	377.7
ZIF-8	18.2	5.5	18.4	27.6	18.7	55.6
MIL-47	20.8	15.7	21.9	87.0	23.2	183.8
UMCM-1	15.5	4.9	15.5	24.7	15.5	49.8
UMCM-150	20.6	11.8	20.3	55.0	20.3	108.9
UMCM-150(N)$_2$	19.5	10.8	19.6	52.5	19.7	105.5

*Unless otherwise noted all data were obtained at 298 K.

Table S34. Geometric surface area, calculated free volume per mass and pore size information of the MOFs investigated in this work

MOF	Geometric Surface Area (m^2/g)	Calculated Free Volume per Mass (cm^3/g)	Pore Size Diameter(s) (Å)
HKUST-1	2134.0	0.801	5.05 / 10.45 / 12.4
Pd(2-pymo)$_2$	533.1	0.385	4.35/ 5.15 / 6.35
IRMOF-1	3562.9	1.319	11.25 / 14.45
IRMOF-3	3365.1	1.204	8.65 / 14.25
MOF-177	4833.0	1.890	10.45
Zn\DOBDC	1324.4	0.490	11.35
Ni\DOBDC	1456.3	0.530	11.05
Co\DOBDC	1508.2	0.543	11.25
Mg\DOBDC	1638.8	0.702	11.35
ZIF-8	1293.9	0.599	10.95
MIL-47	1511.7	0.604	7.35
UMCM-1	4972.7	2.146	10.45 / 14.05 / 23.75
UMCM-150	3236.5	1.186	9.25 / 10.55 / 13.25
UMCM-150(N)$_2$	3110.8	1.168	9.45 / 11.55 / 13.35

Table S35. Surface and free volume density of metal atoms in MOFs with open metal sites

MOF	Surface density (nm^{-2})	Free Volume density (nm^{-3})
Zn\DOBDC	2.798	7.564
Ni\DOBDC	2.655	7.298
Co\DOBDC	2.559	7.109
Mg\DOBDC	3.031	7.074
HKUST-1	1.400	3.730
UMCM-150	0.738	2.015
UMCM-150(N)$_2$	0.764	2.036

6. Acknowledgements and Disclaimer

This project is supported by the U.S. Department of Energy through the National Energy Technology Laboratory, under Award No. DE-FC26-07NT43092. However, any opinions, findings, conclusions, or recommendations expressed herein are those of the author(s) and do not necessarily reflect the views of the DOE. This material is also based upon work supported by the National Science Foundation through TeraGrid resources provided by Purdue University.

References

(1) Chui, S. S. Y.; Lo, S. M. F.; Charmant, J. P. H.; Orpen, A. G.; Williams, I. D. *Science* **1999**, *283*, 1148.

(2) Navarro, J. A. R.; Barea, E.; Salas, J. M.; Masciocchi, N.; Galli, S.; Sironi, A.; Ania, C. O.; Parra, J. B. *Inorg. Chem.* **2006**, *45*, 2397.

(3) Li, H.; Eddaoudi, M.; O'Keeffe, M.; Yaghi, O. M. *Nature* **1999**, *402*, 276.

(4) Eddaoudi, M.; Kim, J.; Rosi, N.; Vodak, D.; Wachter, J.; O'Keeffe, M.; Yaghi, O. M. *Science* **2002**, *295*, 469.

(5) Chae, H. K.; Siberio-Perez, D. Y.; Kim, J.; Go, Y.; Eddaoudi, M.; Matzger, A. J.; O'Keeffe, M.; Yaghi, O. M. *Nature* **2004**, *427*, 523.

(6) Rowsell, J. L. C.; Yaghi, O. M. *J. Am. Chem. Soc.* **2006**, *128*, 1304.

(7) Dietzel, P. D. C.; Panella, B.; Hirscher, M.; Blom, R.; Fjellvag, H. *Chem. Commun.* **2006**, 959.

(8) Dietzel, P. D. C.; Morita, Y.; Blom, R.; Fjellvag, H. *Angew. Chem. Int. Ed.* **2005**, *44*, 6354.

(9) Caskey, S. R.; Wong-Foy, A. G.; Matzger, A. J. *J. Am. Chem. Soc.* **2008**, *130*, 10870.

(10) Park, K. S.; Ni, Z.; Cote, A. P.; Choi, J. Y.; Huang, R. D.; Uribe-Romo, F. J.; Chae, H. K.; O'Keeffe, M.; Yaghi, O. M. *Proc. Natl. Acad. Sci. U. S. A.* **2006**, *103*, 10186.

(11) Barthelet, K.; Marrot, J.; Riou, D.; Ferey, G. *Angew. Chem. Int. Ed.* **2002**, *41*, 281.

(12) Koh, K.; Wong-Foy, A. G.; Matzger, A. J. *Angew. Chem. Int. Ed.* **2008**, *47*, 677.

(13) Wong-Foy, A. G.; Lebel, O.; Matzger, A. J. *J. Am. Chem. Soc.* **2007**, *129*, 15740.

(14) Park, T.; Cychosz, K. A.; Wong-Foy, A. G.; Matzger, A. J. *In Preparation* **2009**.

(15) M. J. Frisch, G. W. T., H. B. Schlegel, G. E. Scuseria, ; M. A. Robb, J. R. C., J. A. Montgomery, Jr., T. Vreven, ; K. N. Kudin, J. C. B., J. M. Millam, S. S. Iyengar, J. Tomasi, ; V. Barone, B. M., M. Cossi, G. Scalmani, N. Rega, ; G. A. Petersson, H. N., M. Hada, M. Ehara, K. Toyota, ; R. Fukuda, J. H., M. Ishida, T. Nakajima, Y. Honda, O. Kitao, ; H. Nakai, M. K., X. Li, J. E. Knox, H. P. Hratchian, J. B. Cross, ; C. Adamo, J. J., R. Gomperts, R. E. Stratmann, O. Yazyev, ; A. J. Austin, R. C., C. Pomelli, J. W. Ochterski, P. Y. Ayala, ; K. Morokuma, G. A. V., P. Salvador, J. J. Dannenberg, ; V. G. Zakrzewski, S. D., A. D. Daniels, M. C. Strain, ; O. Farkas, D. K. M., A. D. Rabuck, K. Raghavachari, ; J. B. Foresman, J. V. O., Q. Cui, A. G. Baboul, S. Clifford, ; J. Cioslowski, B. B. S., G. Liu, A. Liashenko, P. Piskorz, ; I. Komaromi, R. L. M., D. J. Fox, T. Keith, M. A. Al-Laham, ; C. Y. Peng, A. N., M. Challacombe, P. M. W. Gill, ; B. Johnson, W. C., M. W. Wong, C. Gonzalez, and J. A. Pople,. Gaussian 03; Revision C.02 ed.; Gaussian, Inc.: Wallingford, CT, 2004.

(16) Breneman, C. M.; Wiberg, K. B. *J. Comput. Chem.* **1990**, *11*, 361.

(17) Mayo, S. L.; Olafson, B. D.; Goddard, W. A. *J. Phys. Chem.* **1990**, *94*, 8897.

(18) Rappe, A. K.; Casewit, C. J.; Colwell, K. S.; Goddard, W. A.; Skiff, W. M. *J. Am. Chem. Soc.* **1992**, *114*, 10024.

(19) Potoff, J. J.; Siepmann, J. I. *AlChE J.* **2001**, *47*, 1676.

(20) Martin, M. G.; Siepmann, J. I. *J. Phys. Chem. B* **1998**, *102*, 2569.

(21) Frost, H.; Düren, T.; Snurr, R. Q. *J. Phys. Chem. B* **2006**, *110*, 9565.

(22) Snurr, R. Q.; Bell, A. T.; Theodorou, D. N. *J. Phys. Chem.* **1993**, *97*, 13742.

(23) Düren, T.; Millange, F.; Ferey, G.; Walton, K. S.; Snurr, R. Q. *J. Phys. Chem. C* **2007**, *111*, 15350.

(24) Gelb, L. D.; Gubbins, K. E. *Langmuir* **1999**, *15*, 305.

(25) Wang, Q. M.; Shen, D. M.; Bulow, M.; Lau, M. L.; Deng, S. G.; Fitch, F. R.; Lemcoff, N. O.; Semanscin, J. *Microporous Mesoporous Mater.* **2002**, *55*, 217.

(26) Yazaydın, A. Ö.; Benin, A. I.; Faheem, S.A.; Jakubczak, P.; Low, J. J.; Willis, R. R.; Snurr, R. Q. *Chem. Mat.* **2009**, *21*, 1425.

(27) Liang, Z.; Marshall, M.; Chaffe A.L. *Energy & Fuels* **2009**, *23*, 2785.

(28) Cavenati, S.; Grande, C. A.; Rodrigues, A. E. *Ind. Eng. Chem. Res.* **2008**, *47*, 6333.

(29) Chowdhury, P.; Bikkina, C.; Meister, D.; Dreisbahc F.; Gumma, S. *Microporous Mesoporous Mater.* **2009**, *117*, 406.

(30) Huang, L. M.; Wang, H. T.; Chen, J. X.; Wang, Z. B.; Sun, J. Y.; Zhao, D. Y.; Yan, Y. S. *Microporous Mesoporous Mater.* **2003**, *58*, 105.

(31) Millward, A. R.; Yaghi, O. M. *J. Am. Chem. Soc.* **2005**, *127*, 17998.

(32) Kresse, G.; Furthmuller, J. *Comput. Mater. Sci.* **1996**, *6*, 15.

(33) Kresse, G.; Furthmuller, J. *Phys. Rev. B* **1996**, *54*, 11169.

(34) Kresse, G.; Hafner, J. *Phys. Rev. B* **1994**, *49*, 14251.

(35) Kresse, G.; Hafner, J. *Phys. Rev. B* **1993**, *47*, 558.

(36) Perdew, J. P.; Zunger, A. *Phys. Rev. B* **1981**, *23*, 5048.

(37) Kresse, G.; Hafner, J. *J. Phys.: Condens. Matter* **1994**, *6*, 8245.

(38) Vanderbilt, D. *Phys. Rev. B* **1990**, *41*, 7892.